

**Combined Analysis of thin structures:
structure, microstructure, texture, stresses,
phase, nanocrystals ...**

at once in a single approach !

**Daniel Chateigner, L. Lutterotti, M. Morales,
Ph. Boullay**

***IUT-UCBN, CRISMAT-CIMAP
Univ. Trento***

Geo-Bio Center 14th June 2012, Munchen

Structure determination on real (textured) samples

Problem 1

Structure and QTA: correlations ?

$f(g)$ and $|F_h|^2$ are different !

$f(g)$:

- Angularly constrained: $[h_1k_1l_1]^*$ and $[h_2k_2l_2]^*$ make a given angle: more determined if F^2 high
- lot of data (spectra) needed

$|F_h|^2$:

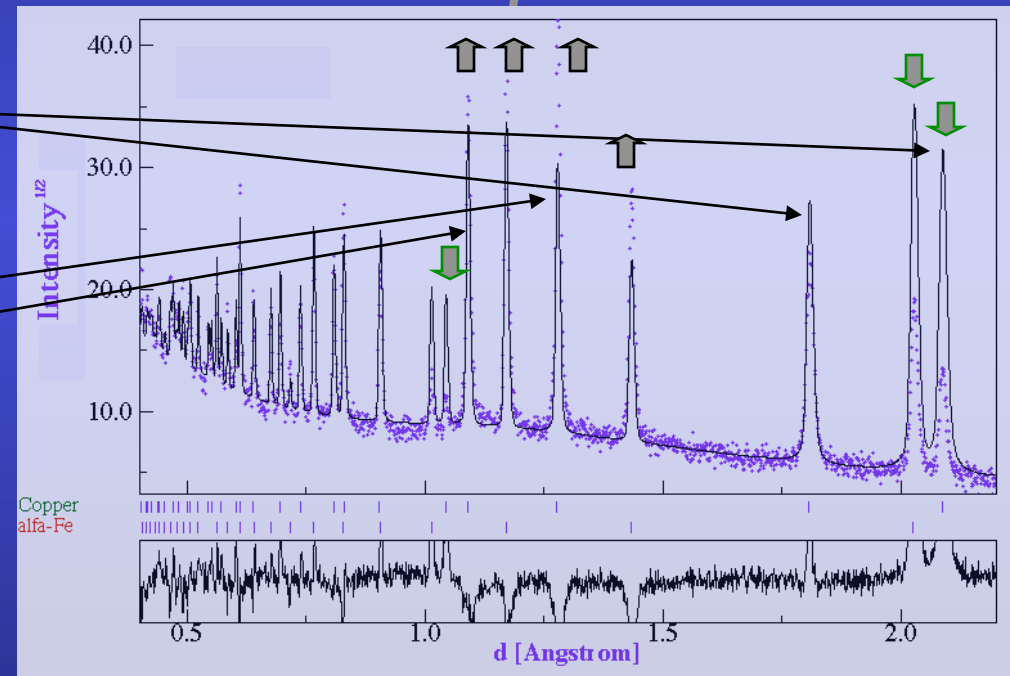
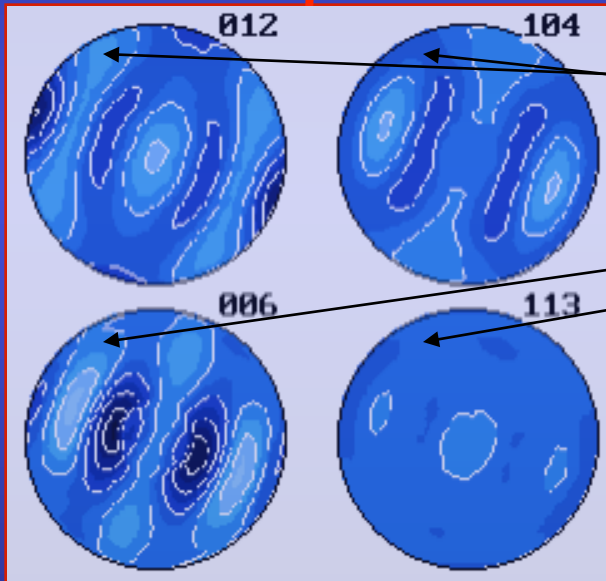
- Position, f_i , and Debye-Waller constrained
- work on the sum of all diagrams on average

Texture from Spectra

Orientation Distribution Function (ODF)

From pole figures

From spectra



Le Bail extraction + ODF: WMV, E-WIMV, Generalized spherical harmonics, components, ADC, entropy maximisation ...

Why not benefit of texture in Structure determination ?

Perfect powders:

- overlaps (intra- and inter- τ)
- no angular constrain
- anisotropy difficult to resc

Single pattern

Single crystals:

- reduced overlaps
 - max angular constrains
- Perfect texture: max anisotropy

Many individual diffracted peaks

Textured powders:

- reduced overlaps
- angular constrain = $f(\text{texture strength})$
- Intermediate anisotropy

Many patterns to measure and analyse

Rietveld-Structure

$$y_c(\mathbf{y}_S, \theta, \eta) = y_b(\mathbf{y}_S, \theta, \eta) + I_0 \sum_{i=1}^{N_L} \sum_{\Phi=1}^{N_\Phi} \frac{v_{i\Phi}}{V_{c\Phi}^2} \sum_h L_p(\theta) j_{\Phi h} |F_{\Phi h}|^2 \Omega_{\Phi h}(\mathbf{y}_S, \theta, \eta) P_{\Phi h}(\mathbf{y}_S, \theta, \eta) A_{i\Phi}(\mathbf{y}_S, \theta, \eta)$$

Texture

$$P_k(\chi, \phi) = \int_{\varphi} f(\mathbf{g}, \varphi) d\varphi$$

- Generalized Spherical Harmonics (Bunge):

$$P_k(\chi, \phi) = \sum_{l=0}^{\infty} \frac{1}{2l+1} \sum_{n=-l}^l k_l^n(\chi, \phi) \sum_{m=-l}^l C_l^{mn} k_n^{*m}(\Theta_k \phi_k)$$

$$f(\mathbf{g}) = \sum_{l=0}^{\infty} \sum_{m,n=-l}^l C_l^{mn} T_l^{mn}(\mathbf{g})$$

- Components (Helming):

$$f(\mathbf{g}) = F + \sum_c I^c f^c(\mathbf{g})$$

- WIMV (William, Imhof, Matthies, Vinel) iterative process:

$$f^{n+1}(\mathbf{g}) = N_n \frac{f^n(\mathbf{g})f^0(\mathbf{g})}{\left(\prod_{\mathbf{h}=1}^I \prod_{m=1}^{M_h} P_{\mathbf{h}}^n(\mathbf{y}) \right)^{\frac{1}{IM_h}}}$$

$$f^0(\mathbf{g}) = N_0 \left(\prod_{\mathbf{h}=1}^I \prod_{m=1}^{M_h} P_{\mathbf{h}}^{\text{exp}}(\mathbf{y}) \right)^{\frac{1}{IM_h}}$$

E-WIMV (Rietveld only):

with $0 < r_n < 1$, relaxation parameter,
 M_h number of division points of the integral
 around k ,
 w_h reflection weight

$$f^{n+1}(\mathbf{g}) = f^n(\mathbf{g}) \prod_{m=1}^{M_h} \left(\frac{P_{\mathbf{h}}(\mathbf{y})}{P_{\mathbf{h}}^n(\mathbf{y})} \right)^{r_n \frac{w_h}{M_h}}$$

- Entropy maximisation (Schaeben):

$$f^{n+1}(\mathbf{g}) = f^n(\mathbf{g}) \prod_{m=1}^{M_h} \left(\frac{P_{\mathbf{h}}(\mathbf{y})}{P_{\mathbf{h}}^n(\mathbf{y})} \right)^{\frac{r_n}{M_h}}$$

- arbitrarily defined cells (ADC, Pawlik): Very similar to E-WIMV, with integrals along path tubes

Residual Stresses shift peaks with γ

Problem 2

Stress and QTA: correlations ? $f(g)$ and $\langle C_{ijkl} \rangle$

$f(g)$:

- Moves the $\sin^2\Psi$ law away from linear relationship
- Needs the integrated peak (full spectra)

strains:

- Measured with pole figures
- needs the mean peak position

Isotropic samples: triaxial, biaxial, uniaxial stress states

Textured samples: Reuss, Voigt, Hill, Bulk geometric mean approaches

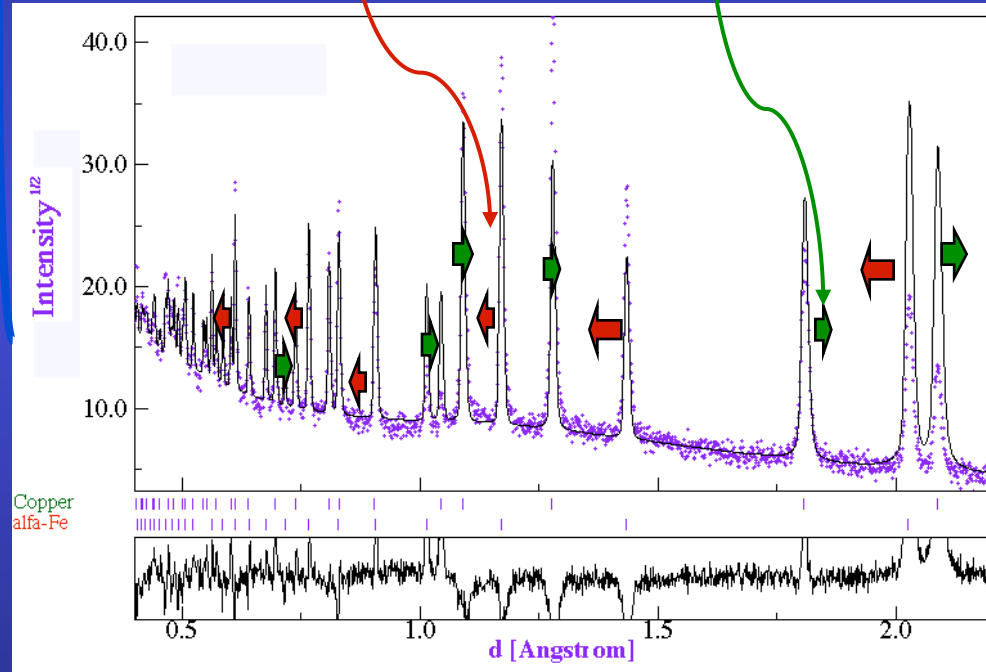
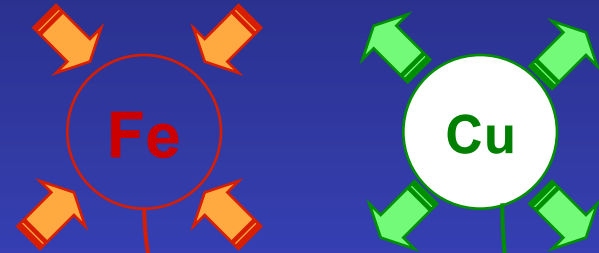
Residual Stresses and Rietveld

- Macro elastic strain tensor (I kind)
- Crystal anisotropic strains (II kind)

C

Macro and micro stresses

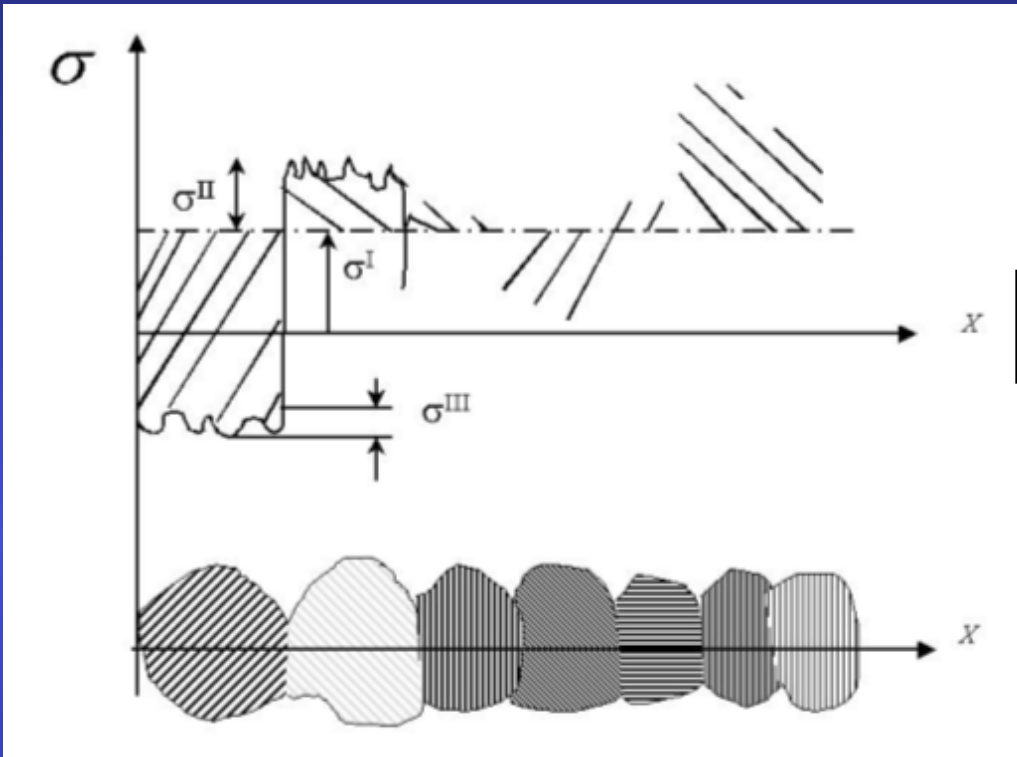
Applied macro stresses



Isotropic samples: triaxial, biaxial, uniaxial stress states

Textured samples: Reuss, Voigt, Hill, Bulk geometric mean approaches

Strain-Stress



$$\boldsymbol{\varepsilon}(\mathbf{X}) = \boldsymbol{\varepsilon}^I + \boldsymbol{\varepsilon}^{II}(\mathbf{X}) + \boldsymbol{\varepsilon}^{III}(\mathbf{X})$$

$$\langle S \rangle_{\text{geo}}^{-1} = \exp \left[- \sum_{m=1}^N v_m \ln S_m \right] = \exp \left[\sum_{m=1}^N v_m \ln S_m^{-1} \right] = \langle S^{-1} \rangle_{\text{geo}} = \langle C \rangle_{\text{geo}}$$

or

$$\langle S \rangle_{\text{geo}}^{-1} = \left[\prod_{m=1}^N S_m^{v_m} \right]^{-1} = \prod_{m=1}^N S_m^{-v_m} = \prod_{m=1}^N (S_m^{-1})^{v_m} = \langle S^{-1} \rangle_{\text{geo}} = \langle C \rangle_{\text{geo}}$$

Layered systems

Problem 3

Layer, Rietveld and QTA: correlations: $f(g)$, thicknesses and structure

$f(g)$:

- Pole figures need corrections for abs-vol
- Rietveld also to correct intensities

layers:

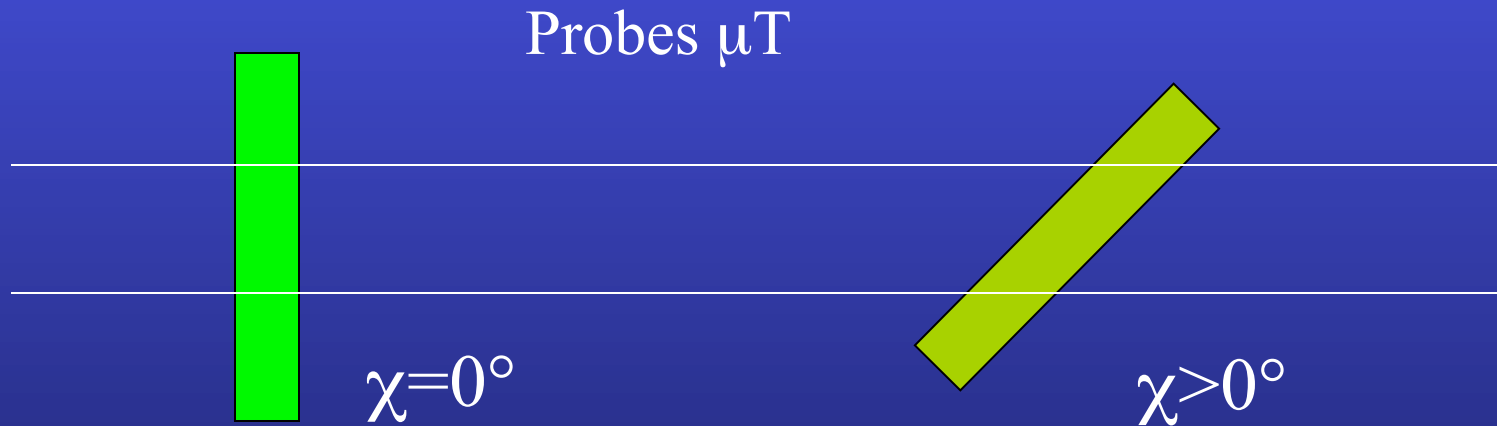
- unknown sample true absorption coefficient μ
- unknown effective thickness (porosity)

Layering

Asymmetric Bragg-Brentano

$$C_{\chi}^{\text{top film}} = g_1 (1 - \exp(-\mu T g_2 / \cos \chi)) / (1 - \exp(-2\mu T / \sin \omega \cos \chi))$$

$$C_{\chi}^{\text{cov. layer}} = C_{\chi}^{\text{top film}} \left(\exp(-g_2 \sum \mu'_i T'_i / \cos \chi) \right) / \left(\exp(-2 \sum \mu'_i T'_i / \sin \omega \cos \chi) \right)$$



Phase and Texture

Problem 4

Phase and QTA: correlations: $f(g)$, S_{Φ}

$f(g)$:

- angular relationships
- plays on individual spectra
- essential to operate on textured sample

S_{Φ} :

- plays on overall scale factor (sum diagram)

Phase analysis

- Volume fraction

$$V_{\Phi} = \frac{S_{\Phi} V_{uc\Phi}^2}{\sum_{\Phi} (S_{\Phi} V_{uc\Phi}^2)_{\Phi}}$$

- Weight fraction

$$m_{\Phi} = \frac{S_{\Phi} Z_{\Phi} M_{\Phi} V_{uc\Phi}^2}{\sum_{\Phi} (S_{\Phi} Z_{\Phi} M_{\Phi} V_{uc\Phi}^2)_{\Phi}}$$

Z = number of formula units

M = mass of the formula unit

V = cell volume

How it works

Le Bail extraction

$$T_{hkl}^k = T_{hkl}^{k-1} \frac{\sum_i I_i^{\text{exp}} S_{hkl}^i}{\sum_i I_i^{\text{calc}} S_{hkl}^i}$$

- Starts with nominal intensities (T_{hkl})
 - Computes the full pattern (I^{calc})
 - Uses the formula to compute next T_{hkl}
 - Cycle the last two steps until convergence
-
- In Maud, options:
 - Only few cycles for texture (3-5) necessary
 - The range for the weighting of the profile can be reduced
 - Background subtracted or not

Structure and Residual Stresses (shift peaks with \mathbf{y})

Problem 5

Stress and cell parameters: correlations: peak positions and C_{ijkl}

Cell parameters:

- Measured at high angles
- Bragg law evolution

strains:

- Measured precisely at high angles
- stiffness-based variation, also with Ψ

Shapes, microstrains, defaults, distributions

Problem 6

Shapes and stress-texture-structure: correlations ?

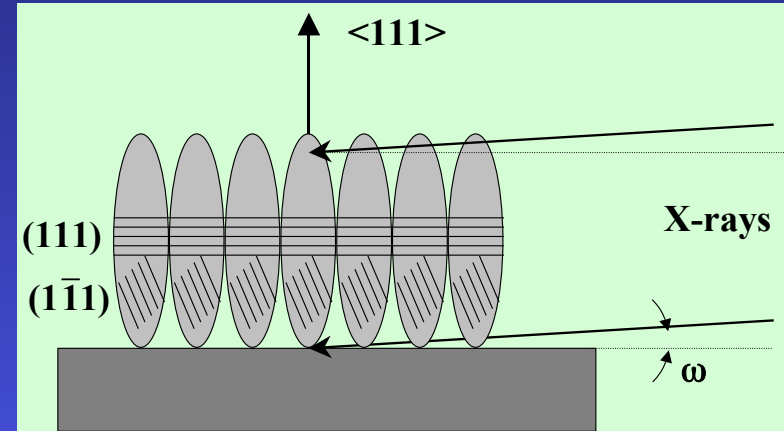
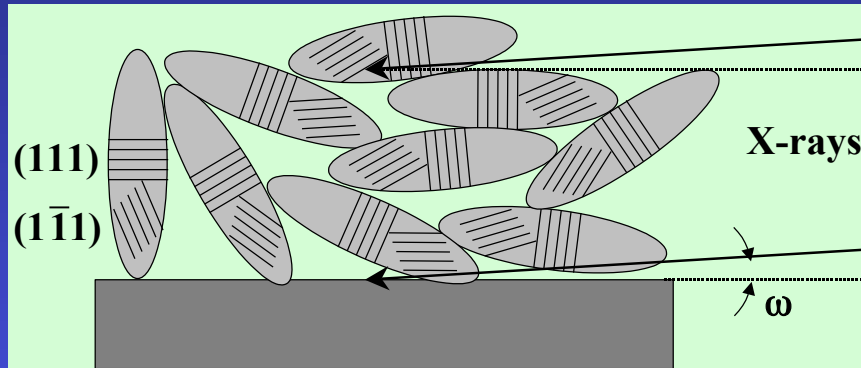
Shapes:

- line broadening problem
- average positions modified
- if anisotropic: modification changes with γ

Stress-texture-structure:

- need “true” peak positions and intensities
- need deconvoluted signals

Anisotropic sizes and microstrains



- Texture helps the "real" mean shape determination
- Determination by peak deconvolution + Popa formalism

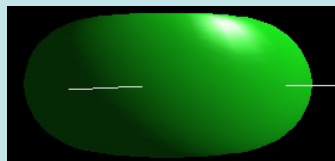
$$\langle R_h \rangle = R_0 + R_1 P_2^0(x) + R_2 P_2^1(x) \cos \varphi + R_3 P_2^1(x) \sin \varphi + R_4 P_2^2(x) \cos 2\varphi + R_5 P_2^2(x) \sin 2\varphi + \dots$$

$$\langle \varepsilon_h^2 \rangle E_h^4 = E_1 h^4 + E_2 k^4 + E_3 \ell^4 + 2E_4 h^2 k^2 + 2E_5 \ell^2 k^2 + 2E_6 h^2 \ell^2 + 4E_7 h^3 k + 4E_8 h^3 \ell + 4E_9 k^3 h + 4E_{10} k^3 \ell + 4E_{11} \ell^3 h + 4E_{12} \ell^3 k + 4E_{13} h^2 k \ell + 4E_{14} k^2 h \ell + 4E_{15} \ell^2 k h$$

$\bar{1}$



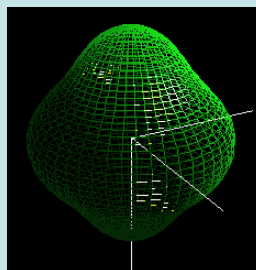
R_0



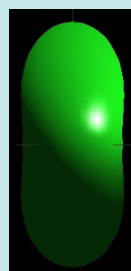
$R_0, R_1 < 0$



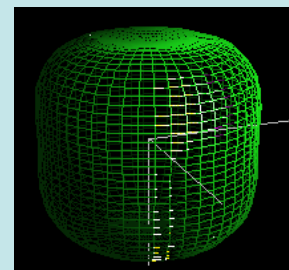
$R_0, R_1 > 0$



$R_0, R_6 > 0$

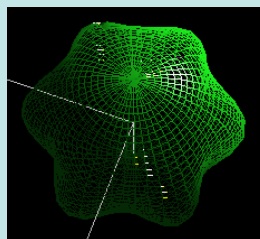


$R_0,$
 R_2 and $R_6 > 0$

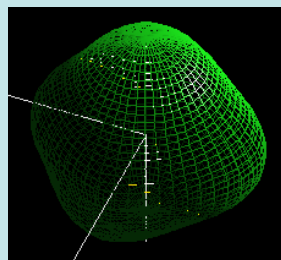


$R_0, R_6 < 0$

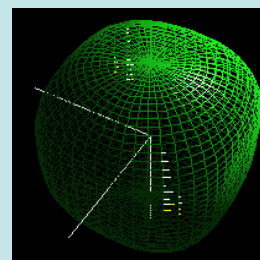
$6/m$



$R_0, R_4 > 0$



$R_0, R_1 > 0$

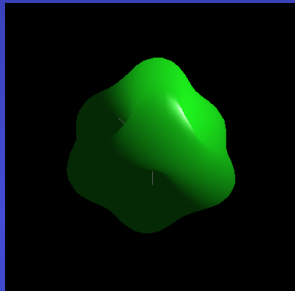


$R_0, R_1 < 0$

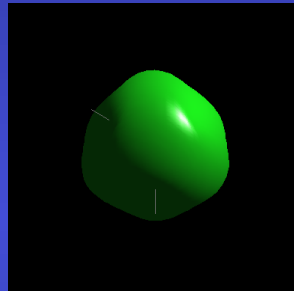
$m\bar{3}m$

Gold thin films

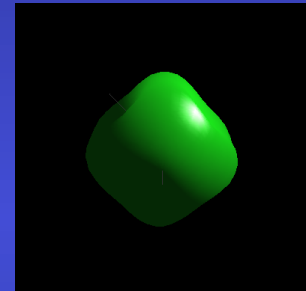
Crystallite size (Å) along	Film thickness					
	10nm	15nm	20nm	25nm	35nm	40nm
[111]	176	153	725	254	343	379
[200]	64	103	457	173	321	386
[202]	148	140	658	234	337	381



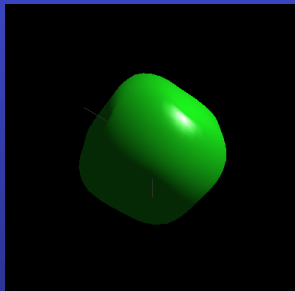
10 nm



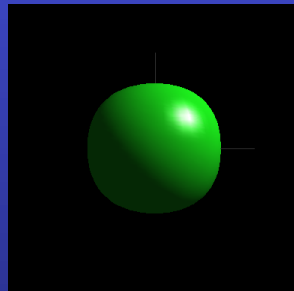
15 nm



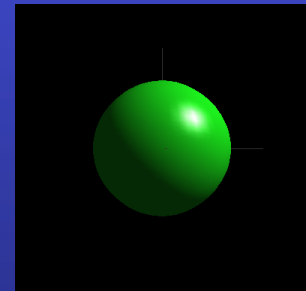
20 nm



25 nm

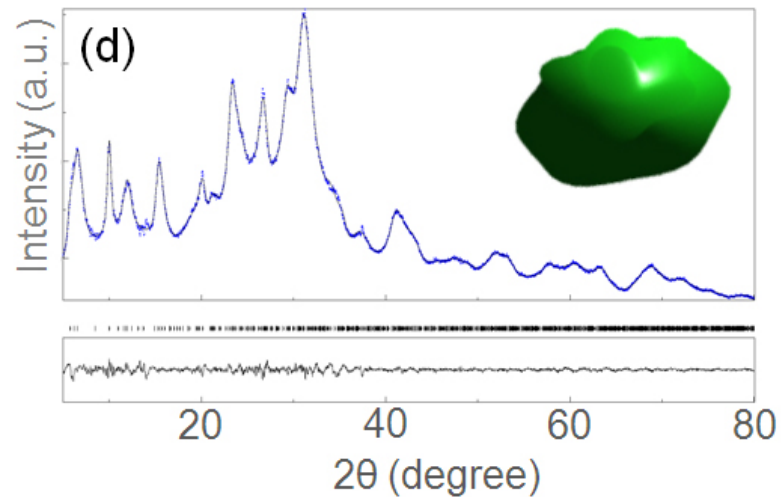
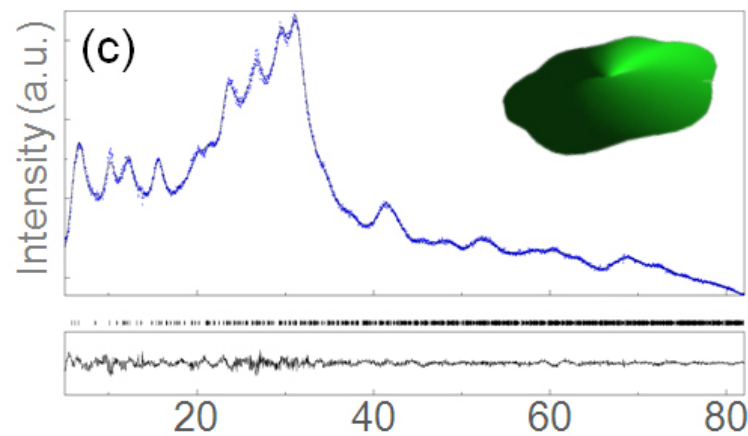
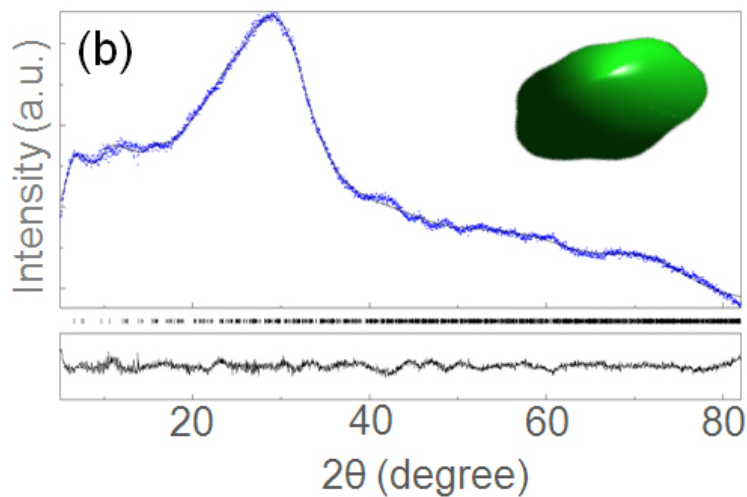
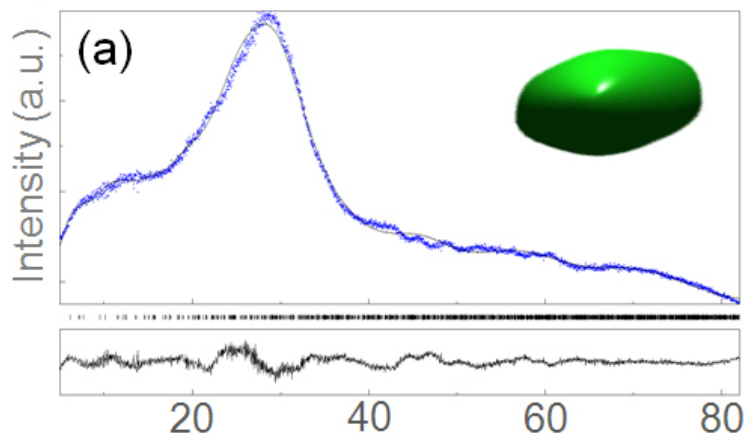


35 nm



40 nm

EMT nanocrystalline zeolite



Ng, Chateigner, Valtchev, Mintova: *Science* **335** (2012) 70

Grinding to powderise another problem !

Grinding: removes angular relationship, adds correlations

Texture:

- not measured
- removed ? hope to get a perfect powder

Strains, defaults, anisotropy ... :

- some removed, some added

Same sample ?

Rare samples ?

Minimum experimental requirements

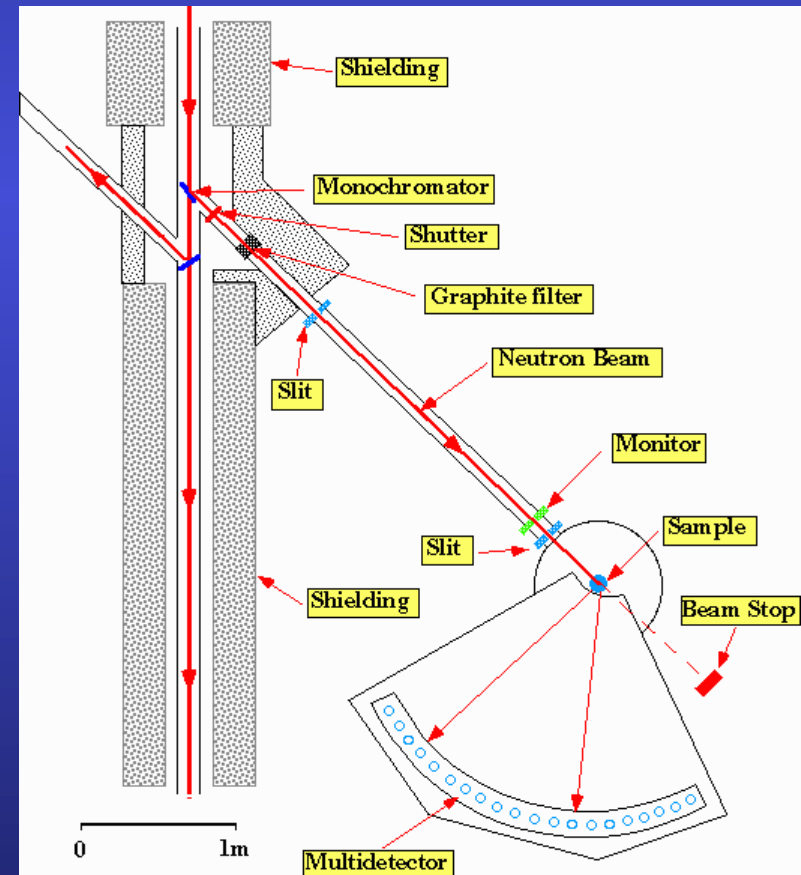
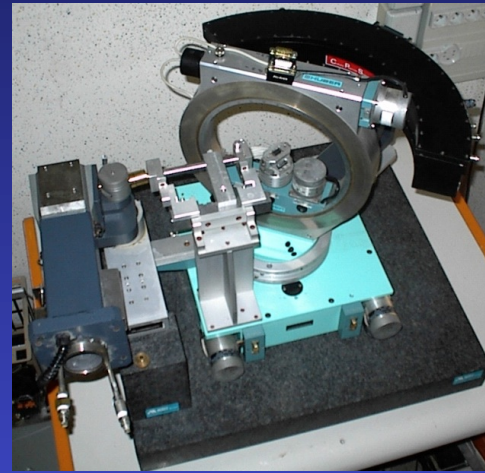
1D or 2D Detector + 4-circle diffractometer
(X-rays and neutrons)
CRISMAT, ILL

+

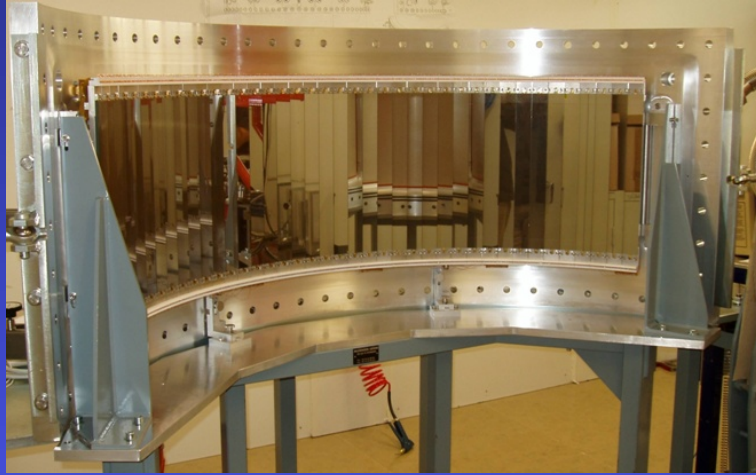
~1000 experiments (2θ diagrams)
in as many sample orientations

+

Instrument calibration
(peaks widths and shapes,
misalignments, defocusing ...)



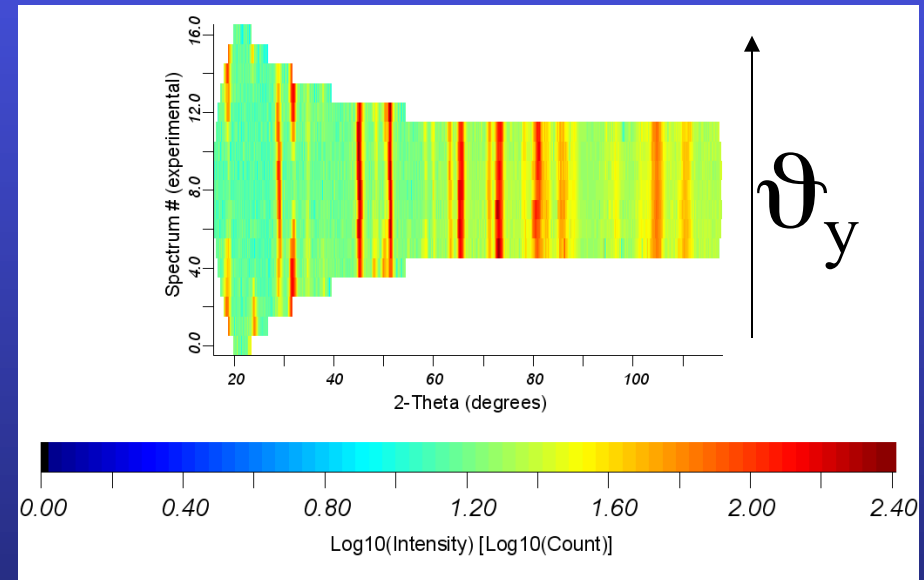
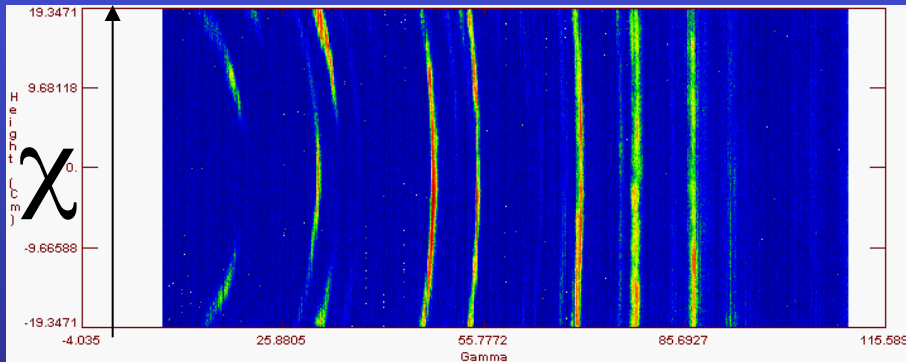
2D Curved Area Position Sensitive Detector



D19 - ILL

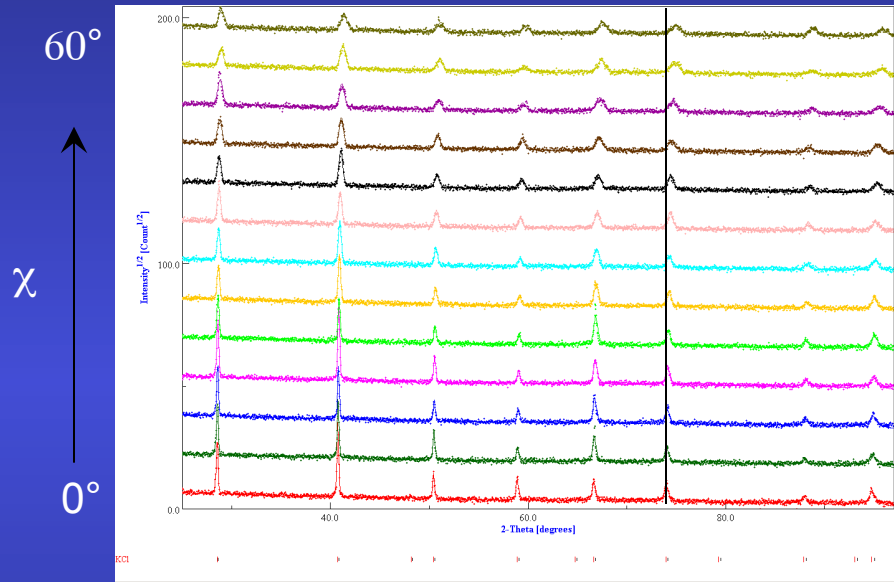
+

~100 experiments (2D Debye-Scherrer diagrams)
in as many sample orientations

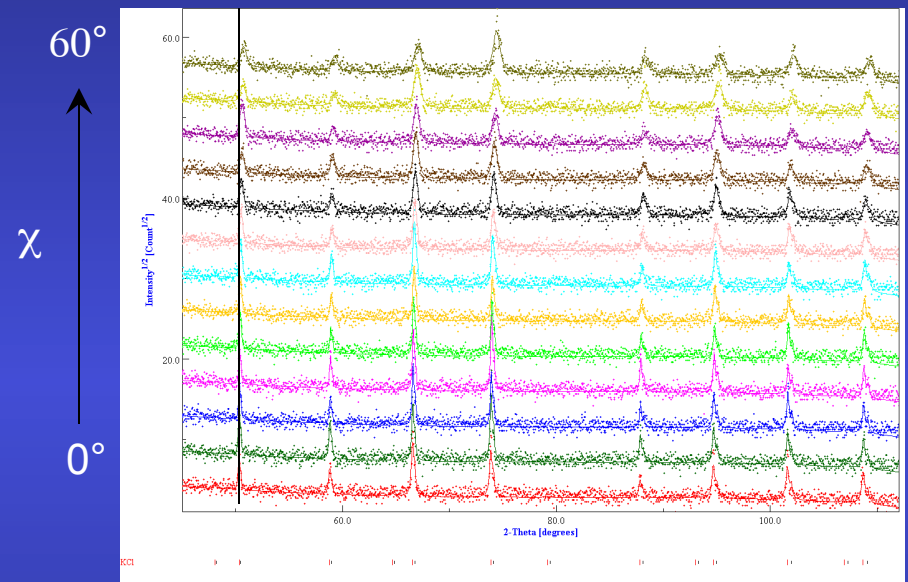


Calibration

$\omega = 20^\circ$



$\omega = 40^\circ$



KCl, LaB₆ ...



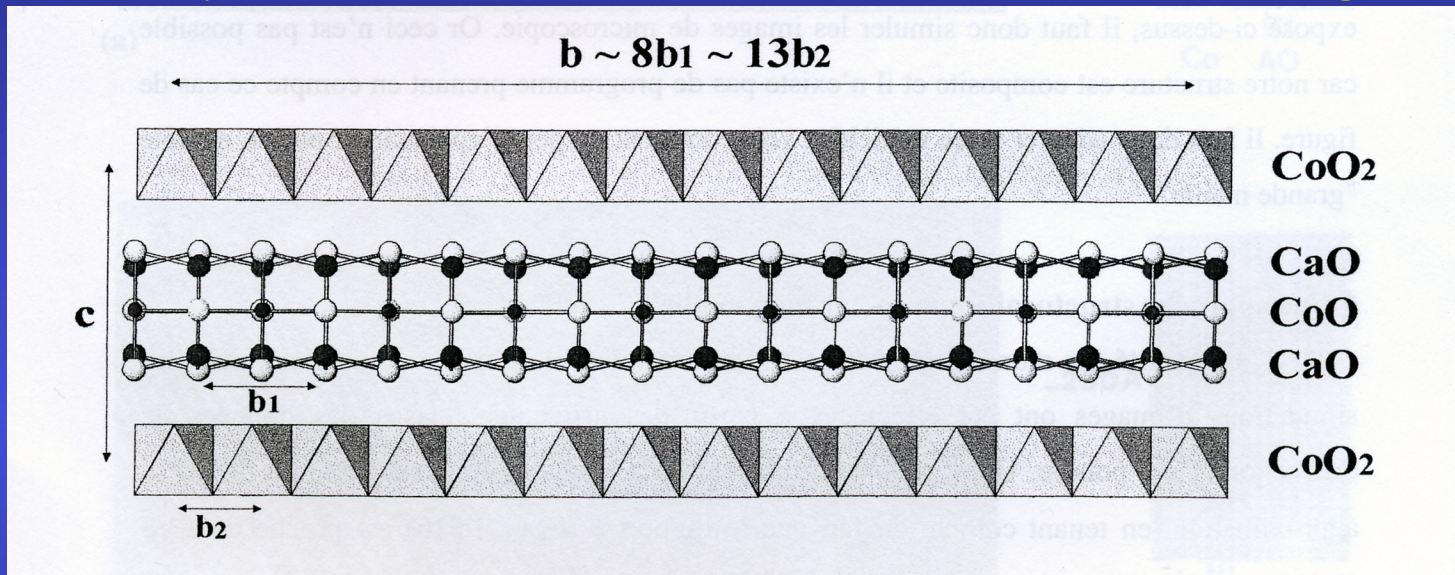
FWHM (ω , χ , 2θ , η ...)
2 θ shift
gaussianity
asymmetry
misalignments ...

Minimization algorithms

- Can be fully used in the method (everywhere)
- **Marquardt Least Squares** (based on steepest decrease and Gauss-Newton)
 - Efficient, best with few parameters, near the solution
- **Evolutionary computation** (or genetic algorithm)
 - Slow, not efficient, requires a lot of resources
 - Unlimited number of parameters
 - Can start far from the solution
- **Simulated annealing** (the solution proceed like a random walk, but the walking step decreases as temperature decreases)
 - In between the Marquardt and evolutionary algorithms
- **Simplex** (generates $n+1$ starting solutions as vertices of a polygon, n number of parameters, and contract/expand the polygon around the minima)
 - Slow on convergence
 - Remains close to the solution, but explore more minima with respect to the Marquardt

Ca₃Co₄O₉ thermoelectrics

Ca₃Co₄O₉: Misfit lamellar and modulated Structure, with high thermopower



Two monoclinic sub-systems:

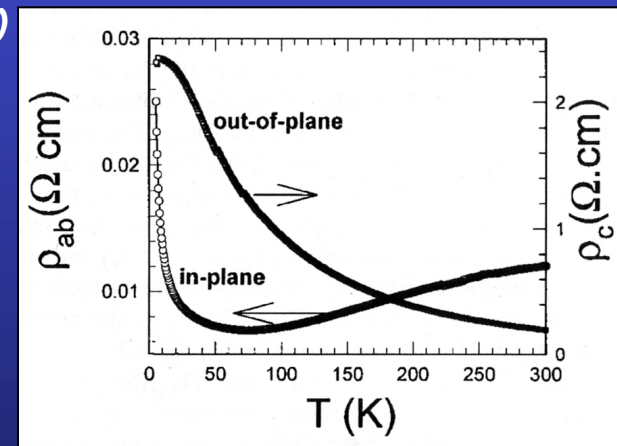
S1 with $a \sim 4.8\text{\AA}$, $b_1 \sim 4.5\text{\AA}$, $c \sim 10.8\text{\AA}$ et $\beta \sim 98^\circ$ (NaCl-type)

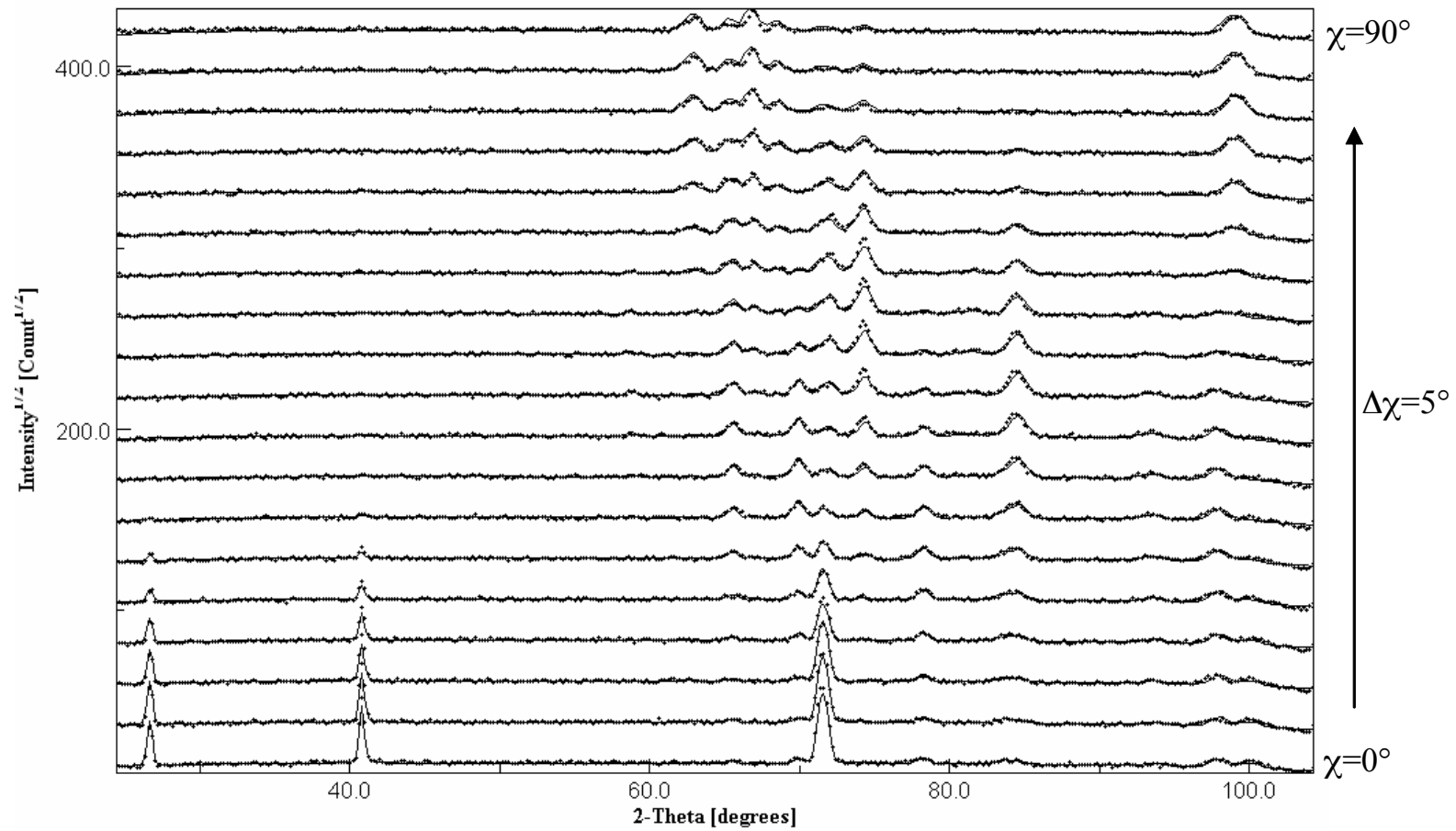
S2 with $a \sim 4.8\text{\AA}$, $b_2 \sim 2.8\text{\AA}$, $c \sim 10.8\text{\AA}$ et $\beta \sim 98^\circ$ (CdI₂-type)

$$\Gamma = \sigma_{ab} / \sigma_c \sim 10$$



Texture



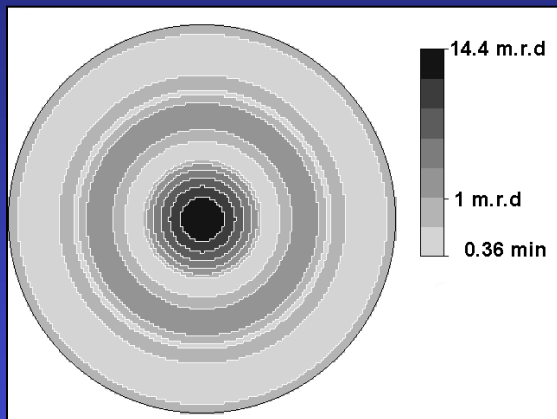


Supercell

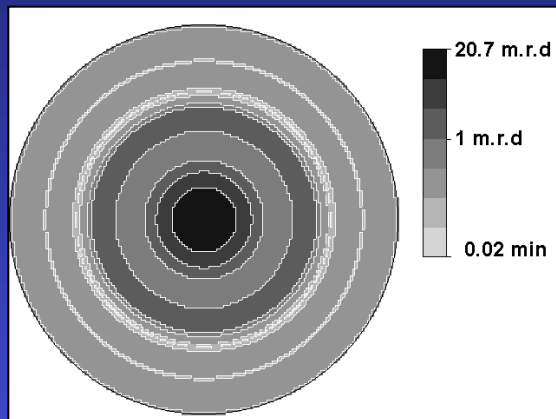


RP=19.7%, Rw=11.9%

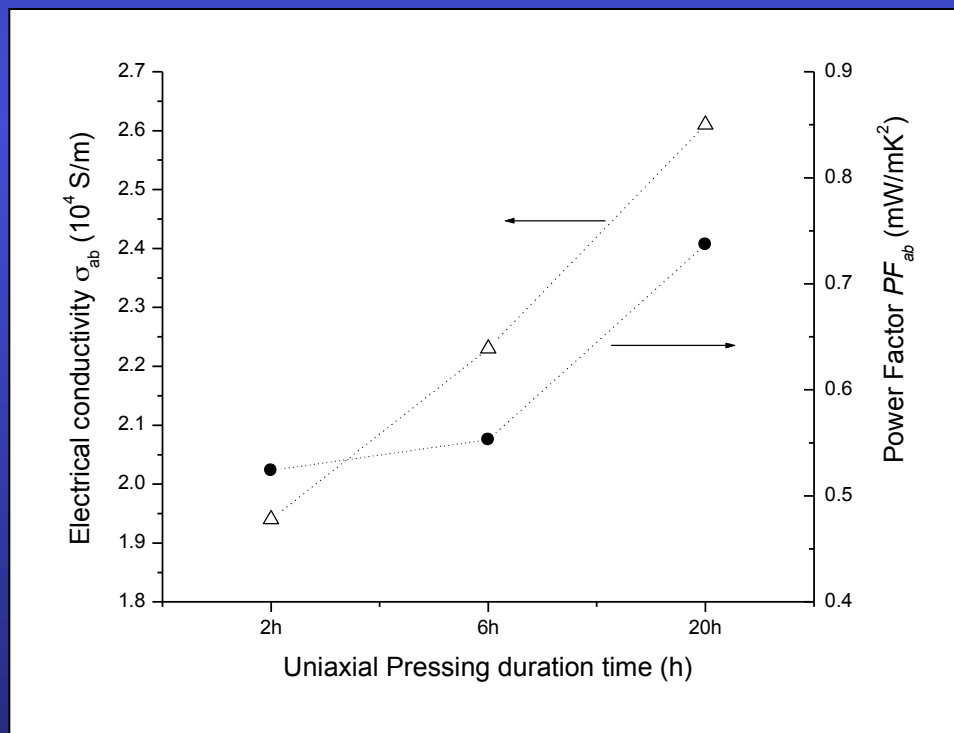
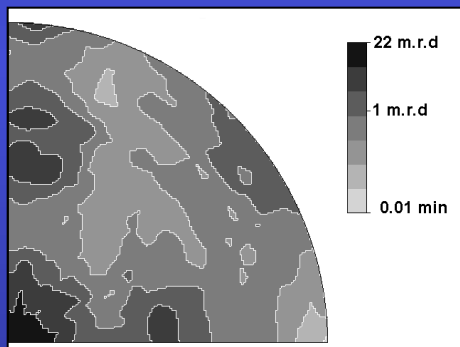
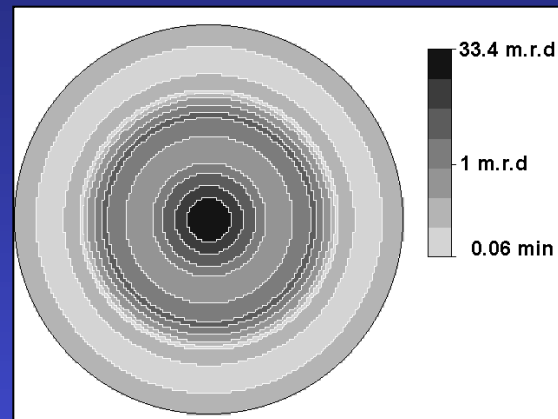
9.8 MPa for 2 h



19.6 MPa for 6 h



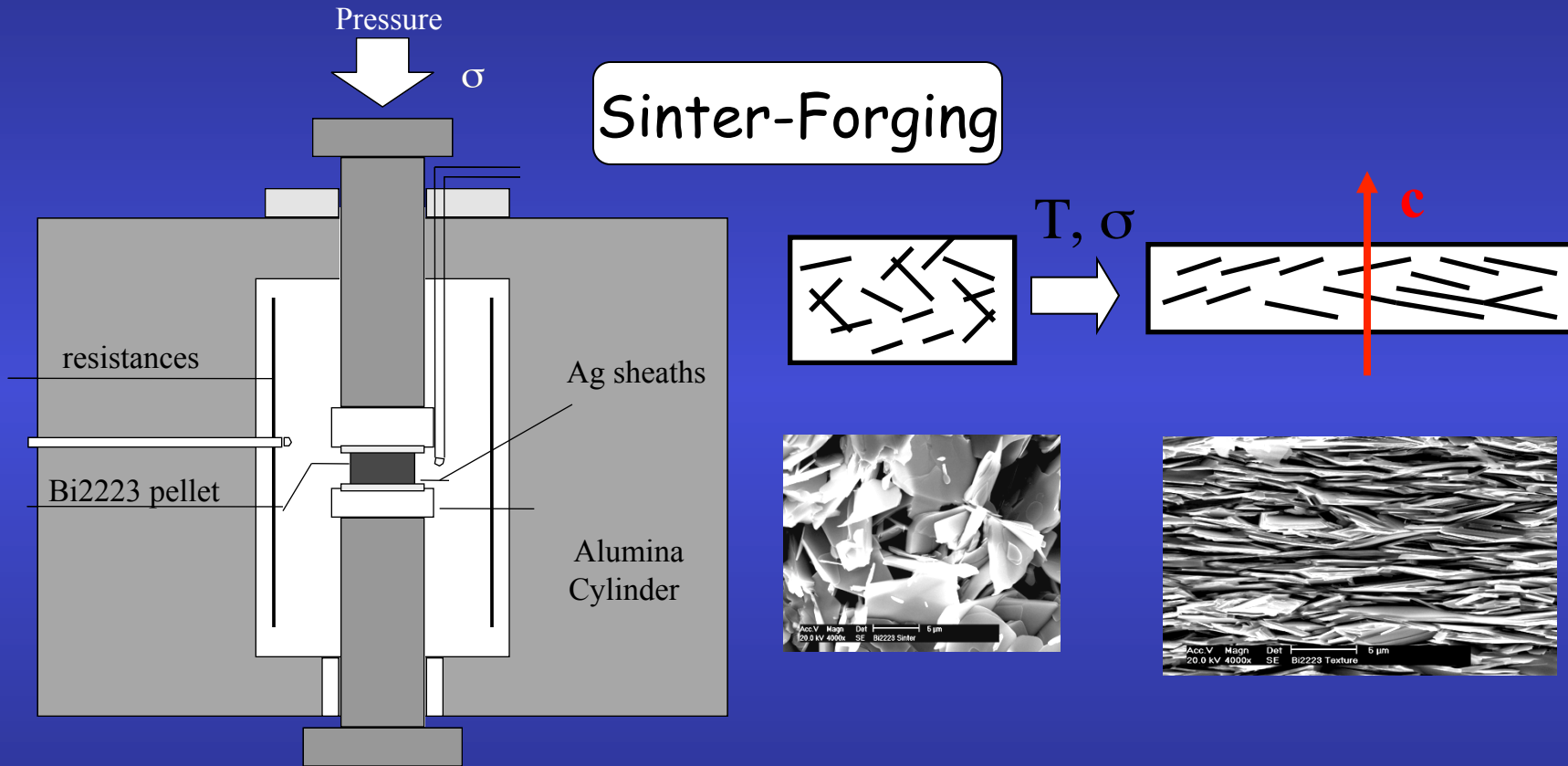
19.6 MPa for 20 h



Templated Growth Method

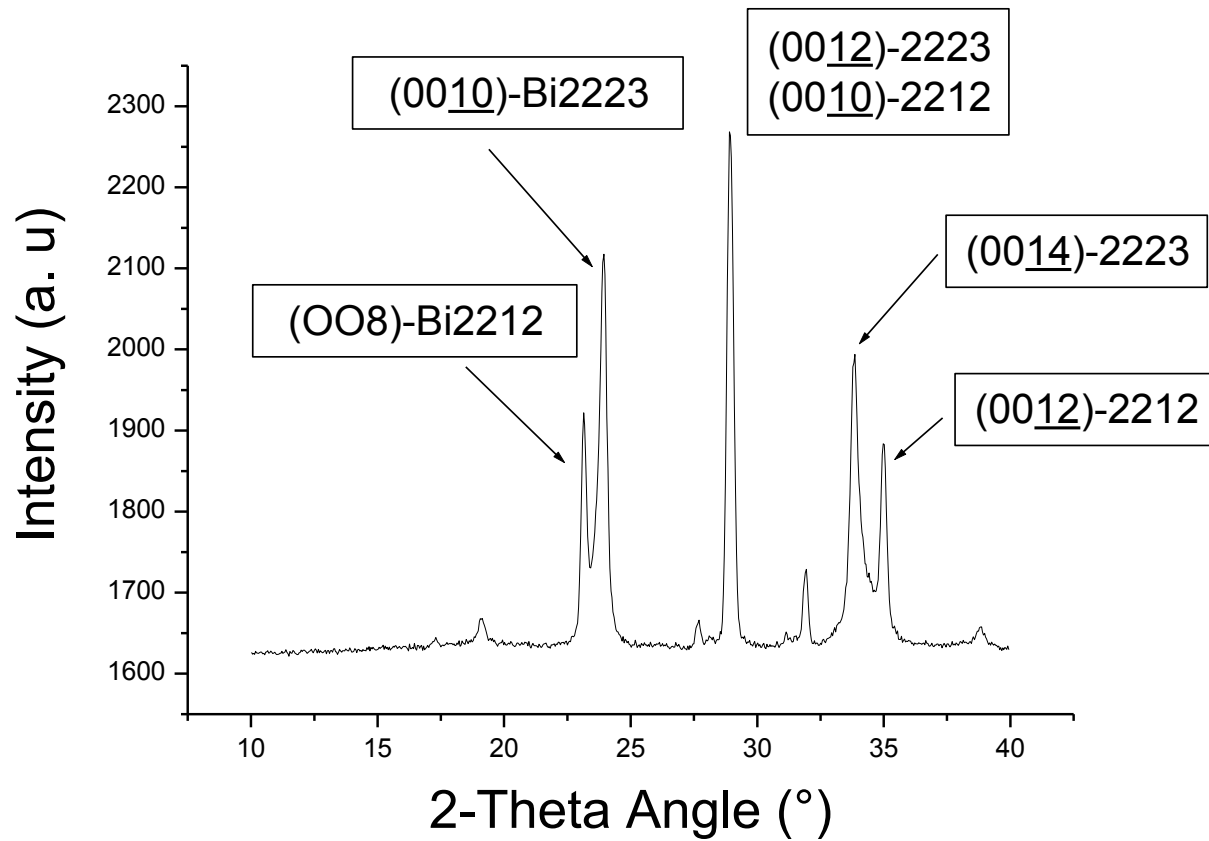
Bi2223 compounds

E. Guilmeau, PhD

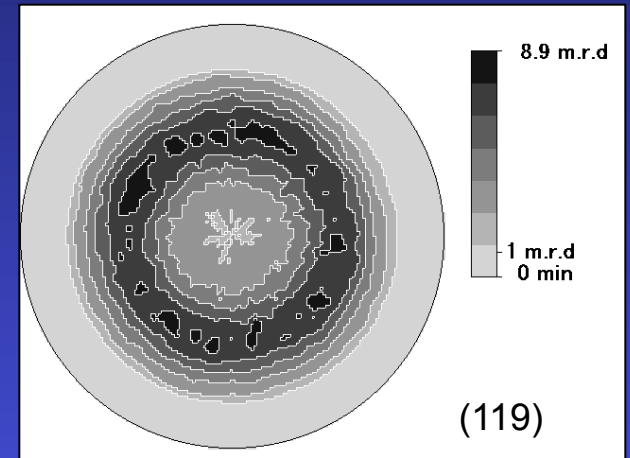
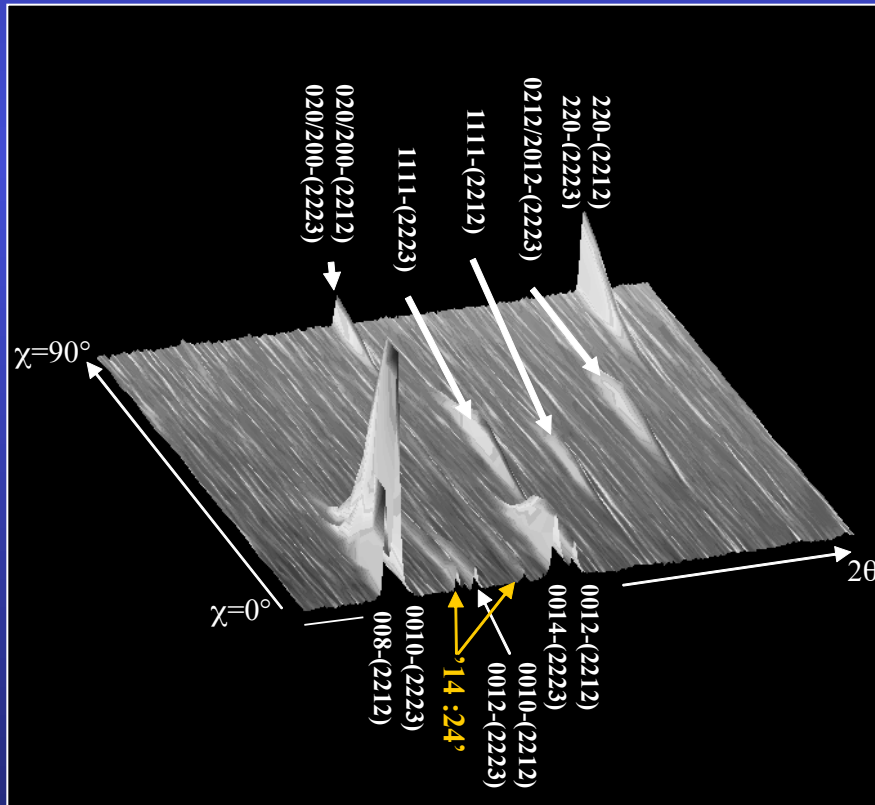


Grain alignment \Rightarrow $\nearrow J_c$

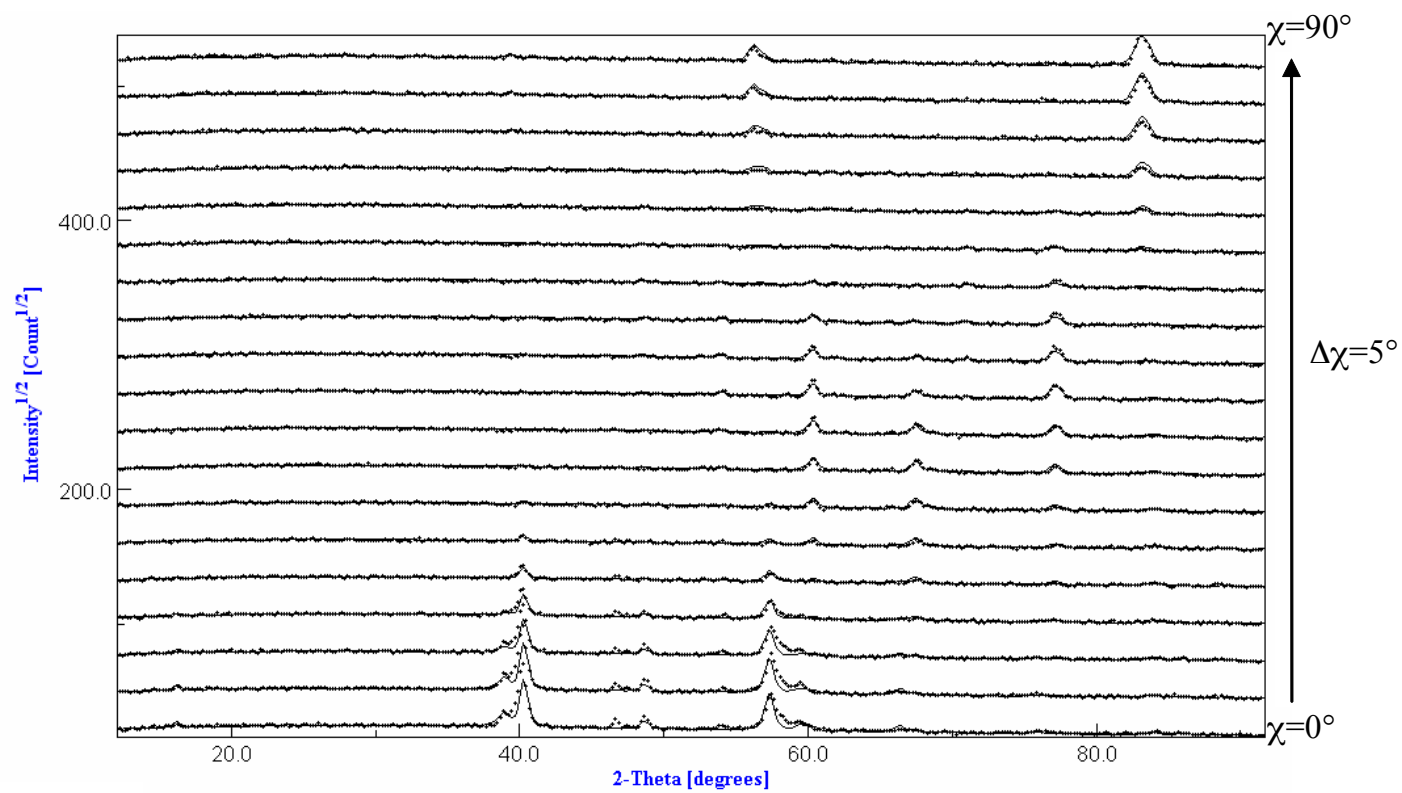
(00 l) Texture



Combined Analysis



- Neutrons
- Sample: $\sim 70 \text{ mm}^3$
- 2θ patterns for $\chi=0^\circ$ to 90°
- No φ rotation (fibre texture).



2223
2212



$R_w=9.12$
 $RP=16.24$

Effect of the sinter-forging treatment on the texture development, crystal growth, transport properties

Sinter-forging dwell time (h)	Orientation Distribution Max (m.r.d.)		% Bi2223	Cell parameters (Å)		Crystallite size Bi2223 (nm)	Rb (%)	Rw (%)	Rexp (%)	RP0 (%)	RP1 (%)	J_c (A/cm ²)
	Bi2212	Bi2223		Bi2223	Bi2212							
20	21.8	20.7	59.9±1.3	a=5.419(3) b=5.391(3) c=37.168(3)	a=5.414(3) b=5.393(3) c=30.800(3)	205±7	7.56	11.1	4.55	17.74	10.56	12500
50	24.1	24.4	72.9±2.9	a=5.419(3) b=5.408(3) c=37.192(3)	a=5.416(3) b=5.396(3) c=30.806(3)	273±10	7.54	11.37	4.58	17.05	11.04	15000
100	31.5	25.2	84.4±4.6	a=5.410(3) b=5.405(3) c=37.144(3)	a=5.412(3) b=5.403(3) c=30.752(3)	303±10	5.4	8.04	3.69	13.54	9.31	19000
150	65.4	27.2	87.0±4.1	a=5.417(3) b=5.403(3) c=37.199(3)	a=5.413(3) b=5.407(3) c=30.792(3)	383±13	6.13	9.12	4.8	16.24	12.25	20000



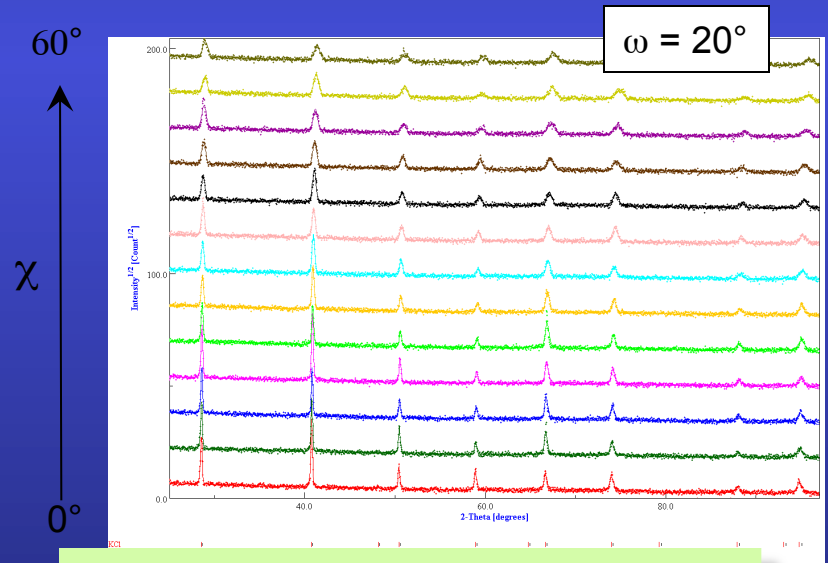
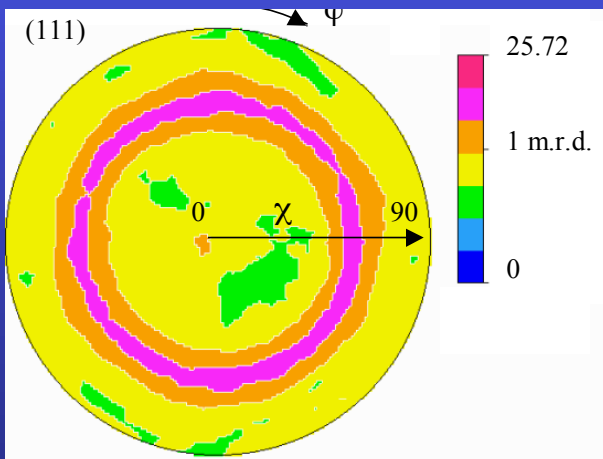
Ferroelectric PCT films

J. Ricote, Madrid

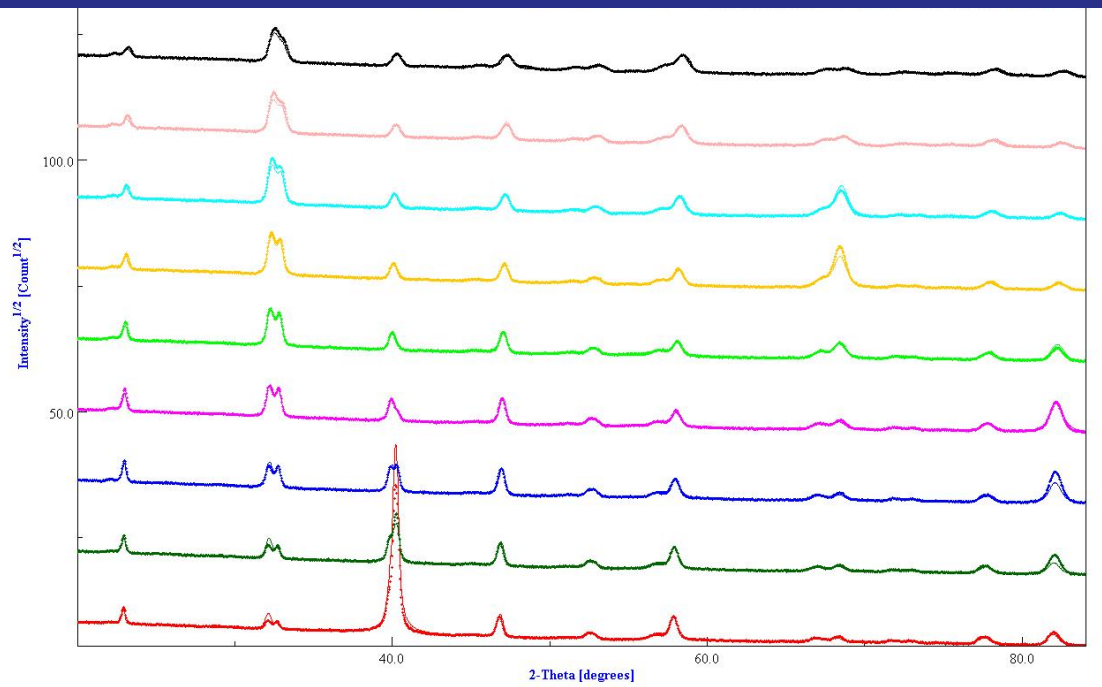
thin films:

$(\text{Ca}_{0.24}\text{Pb}_{0.76})\text{TiO}_3$ sol-gel synthesised solutions deposited by spin coating on a substrate of $\text{Pt}/\text{TiO}_2/\text{Si}$, with and without a treatment at 650°C for 30 min.

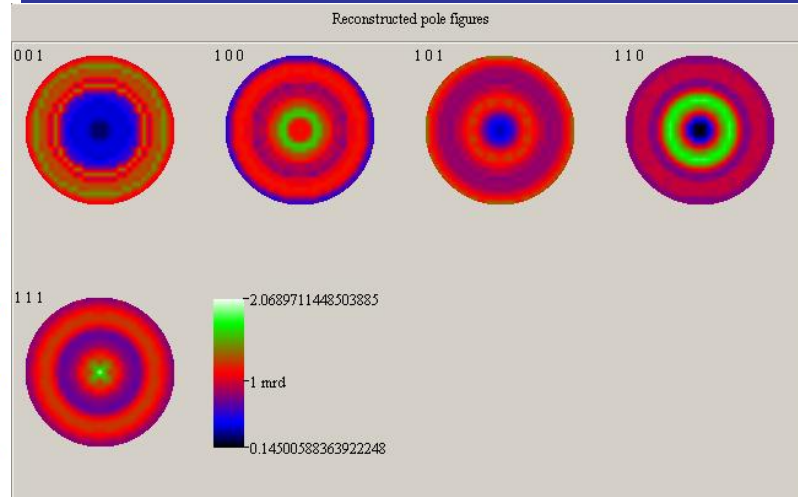
All films are crystallised at 700°C for 50 s by Rapid Thermal Processing (RTP; $30^\circ\text{C}/\text{s}$). A series is also recrystallised at 650°C for 1 to 3 h.



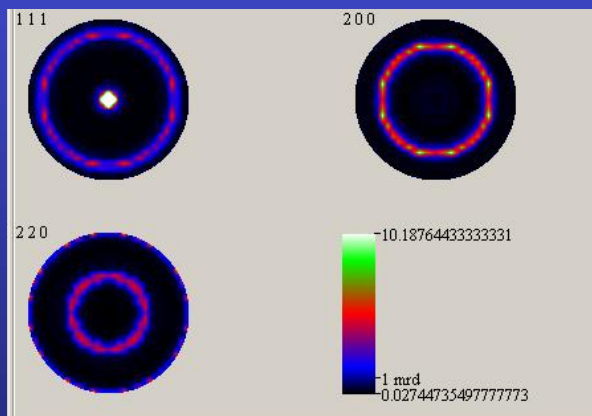
Refinement of individual spectra



PCT



Pt

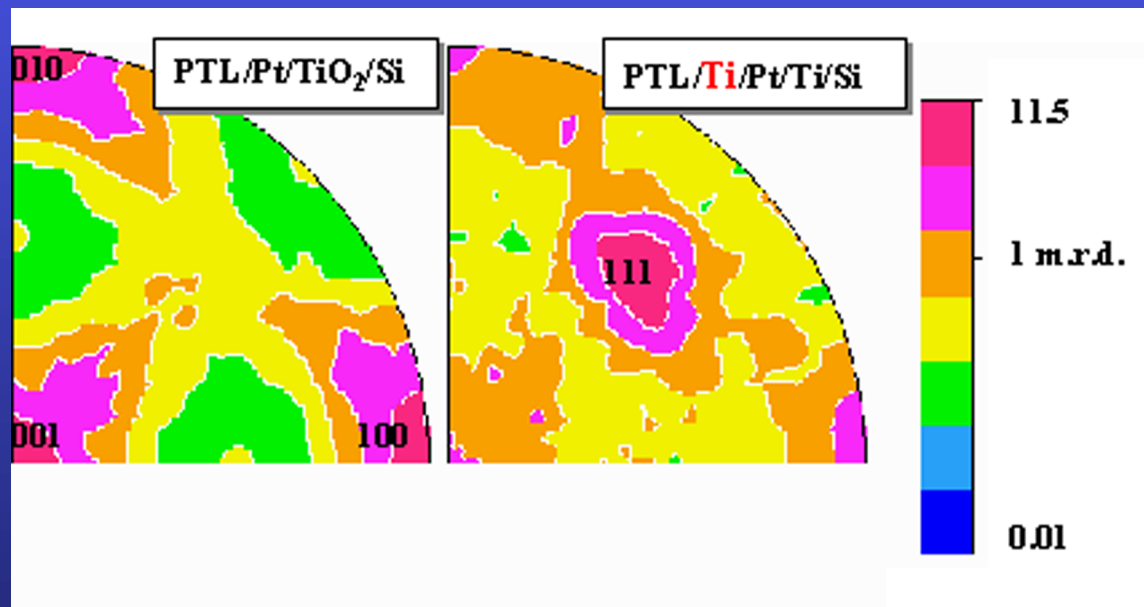


$a = 3.9108(1) \text{ \AA}$
 $T = 457(3) \text{ \AA}$
 $t_{\text{iso}} = 458(3) \text{ \AA}$
 $\epsilon' = 0.0032(1) \text{ rms}$

$a = 3.9156(1) \text{ \AA}$
 $c = 4.0497(3) \text{ \AA}$
 $T = 2525(13) \text{ \AA}$
 $t_{\text{iso}} = 390(7) \text{ \AA}$
 $\epsilon = 0.0067(1) \text{ rms}$

$R_W = 13\%$; $R_B = 12\%$; $R_{\text{exp}} = 22\%$.(Rietveld)
 $R_W = 5\%$; $R_B = 6\%$ (E-WIMV)

Atom	Occupancy	x	y	z
Pb	0.76	0.0	0.0	0.0
Ca	0.24	0.0	0.0	0.0
Ti	1.0	0.5	0.5	0.477(2)
O1	1.0	0.5	0.5	0.060(2)
O2	1.0	0.0	0.5	0.631(1)

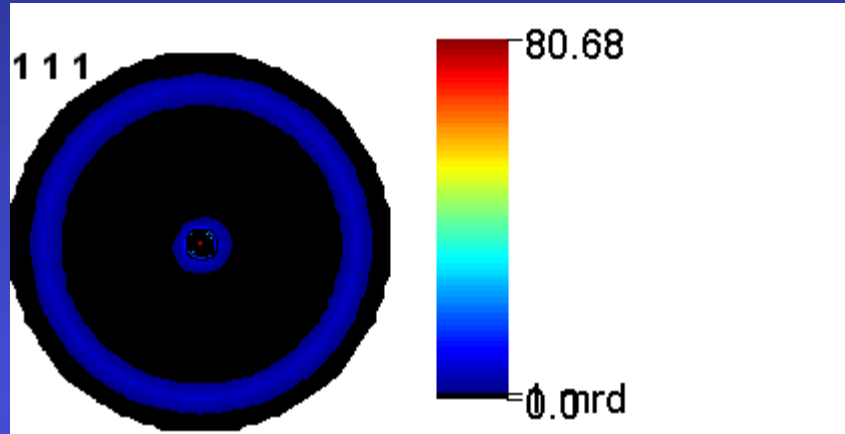


Compliance coefficients [10 ⁻³ GPa ⁻¹]	PbTiO ₃ single crystal (data set A)	Film random orientation	PCT-Si <001> contrib.≈17%	PLT <001> contrib.≈49%	PCT-Mg <001> contrib.≈68%
S ₁₁	6.5	10.1	10.5	10.0	9.7
S ₂₂	6.5	10.0	10.5	10.0	9.7
S ₃₃	33.3	9.8	9.0	10.3	11.3
S ₄₄	14.5	13.2	12.8	12.9	13.1
S ₅₅	14.5	13.2	12.8	13.0	13.1
S ₆₆	9.6	13.4	14.0	13.5	12.7
S ₁₂	-0.35	-3.3	-3.5	-3.2	-3.0
S ₂₁	-0.35	-3.3	-3.5	-3.2	-3.0
S ₁₃	-7.1	-3.2	-3.1	-3.4	-3.6
S ₃₁	-7.1	-3.2	-3.1	-3.4	-3.6
S ₂₃	-7.1	-3.2	-3.1	-3.4	-3.6
S ₃₂	-7.1	-3.2	-3.1	-3.4	-3.6
S ₃₃ /S ₁₁	5.1	0.97	0.86	1.03	1.16
S ₁₃ /S ₁₂	20.3	0.97	0.89	1.06	1.20

Geometric mean average + biaxial stress state

Ferroelectric PMN-PT films

J. Ricote, DMF-Madrid



Pt

$$a = 3.91172(1) \text{ \AA}$$

$$T = 583(5) \text{ \AA}$$

$$t_{\text{iso}} = 960(1) \text{ \AA}$$

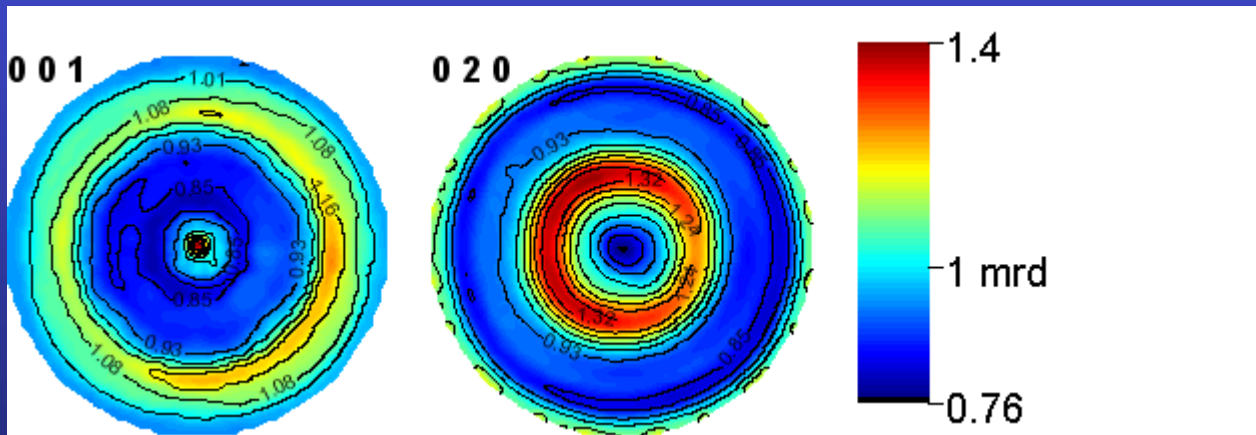
$$\varepsilon = 0.0032(1) \text{ rms}$$

$$\sigma_{11} = 0.639(1) \text{ GPa}$$

$$\sigma_{22} = 0.651(1) \text{ GPa}$$

$$\sigma_{12} = -0.009(1) \text{ GPa}$$

$\text{Pb}_{0.7}(\text{Mg}_{1/3}\text{Nb}_{2/3})\text{O}_3\text{-Pb}_{0.3}\text{TiO}_3 / \text{TiO}_2 / \text{Pt} / \text{Si-(100)}$



$$a = 5.67858(9) \text{ \AA}$$

$$b = 5.69038(9) \text{ \AA}$$

$$c = 3.99558(4) \text{ \AA}$$

$$\beta = 90.392(1) \text{ \AA}$$

$$T = 1322(9) \text{ \AA}$$

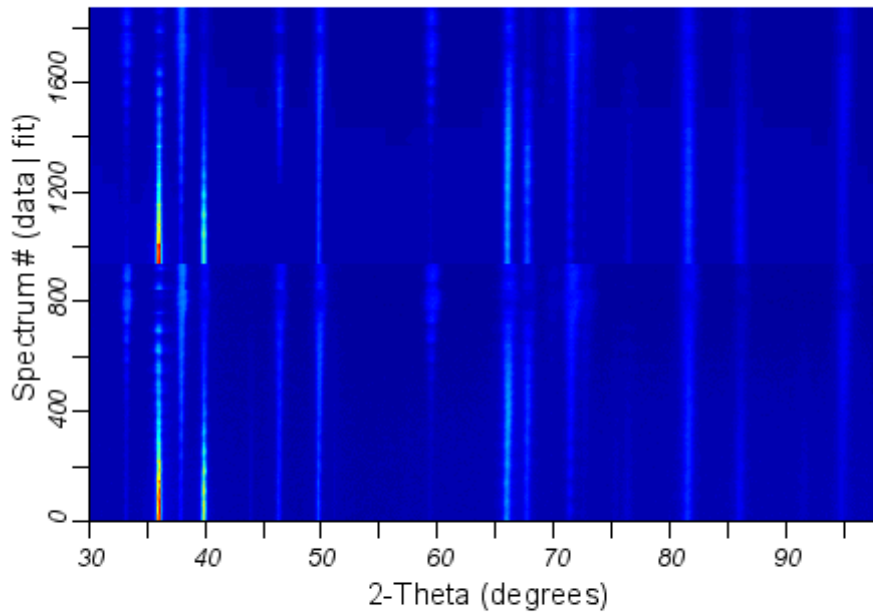
$$t_{\text{iso}} = 1338(2) \text{ \AA}$$

$$\varepsilon = 0.0067(1) \text{ rms}$$

AIN/Pt/TiO_x/Al₂O₃/Ni-Co-Cr-Al

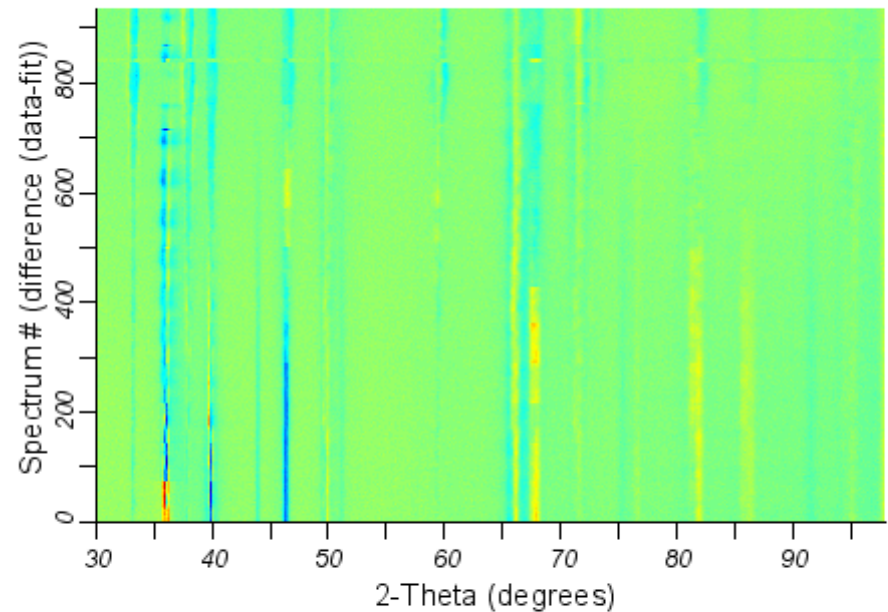
2D Multiplot for Data 05_37P64

measured data and fit



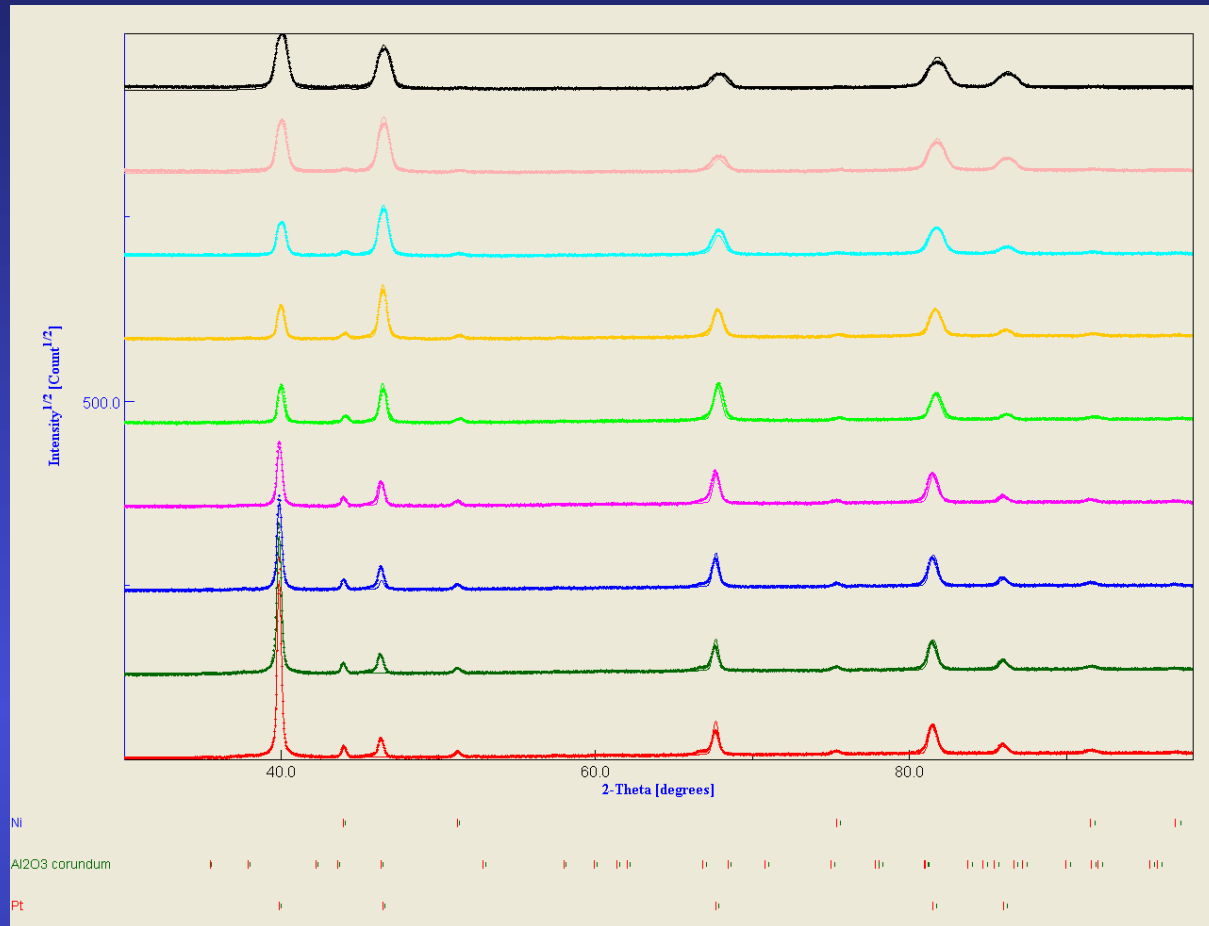
2D difference plot for Data 05_37P64

difference data - fit

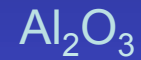


Rw (%) = 24.120445
Rexp (%) = 5.8517213

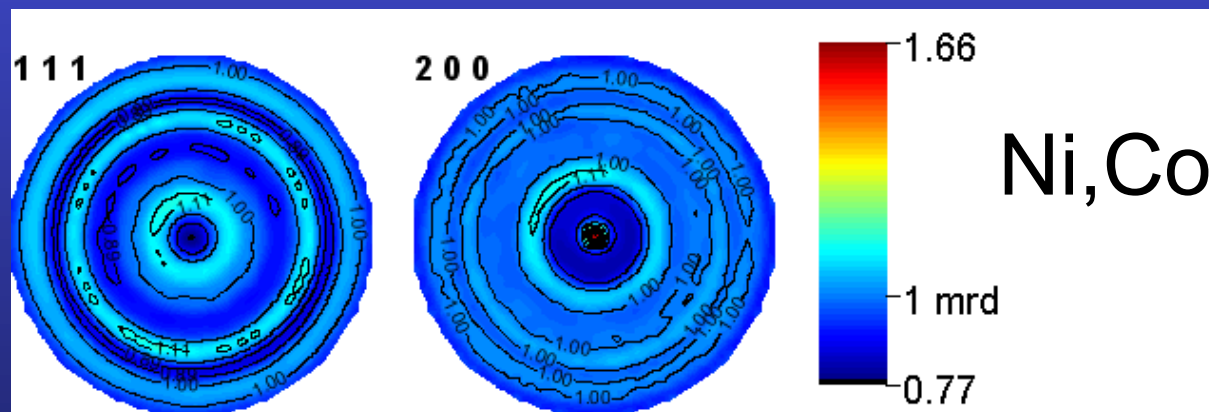
T(AIN) = 14270(3) nm
T(Pt) = 430(3) nm



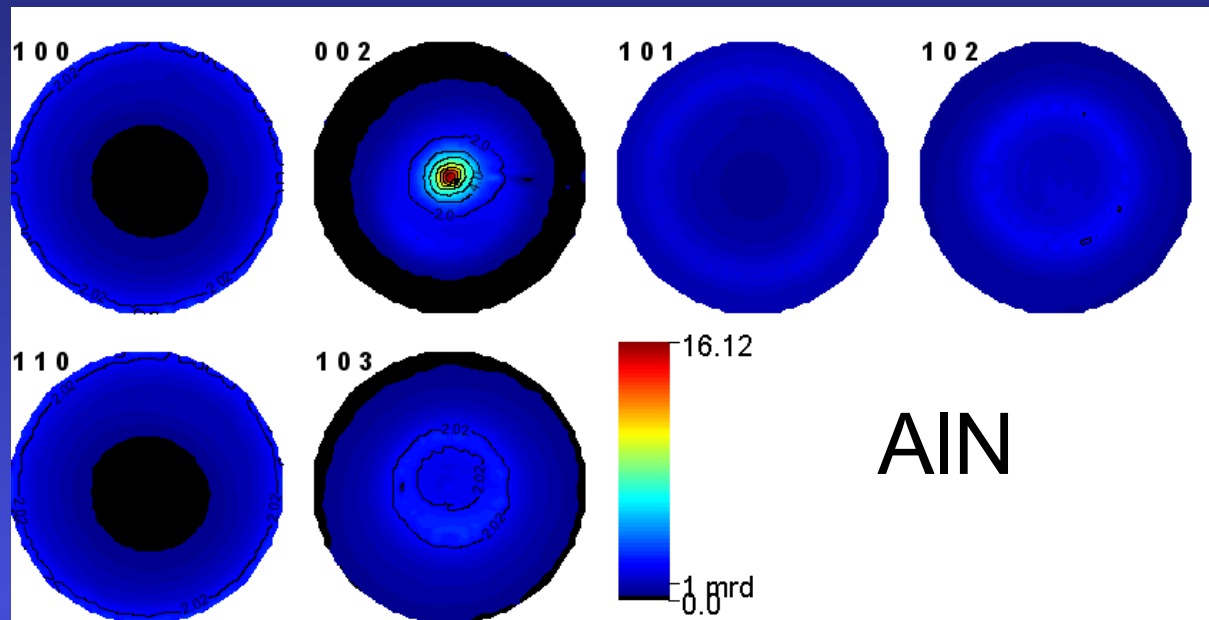
(χ, φ) randomly
selected diagrams



$a = 4.7562(6) \text{ \AA}$
 $c = 12.875(3) \text{ \AA}$
 $T = 7790(31) \text{ nm}$
 $\langle t \rangle = 150(2) \text{ \AA}$
 $\langle \varepsilon \rangle = 0.008(3)$



$a = 3.569377(5) \text{ \AA}$
 $\langle t \rangle = 7600(1900) \text{ \AA}$
 $\langle \varepsilon \rangle = 0.00236(3)$
 $\sigma_{11} = -328(8) \text{ MPa}$
 $\sigma_{22} = -411(9) \text{ MPa}$



Rw (%) = 4.1

$a = 3.11203(1) \text{ \AA}$

$c = 4.98252(1) \text{ \AA}$

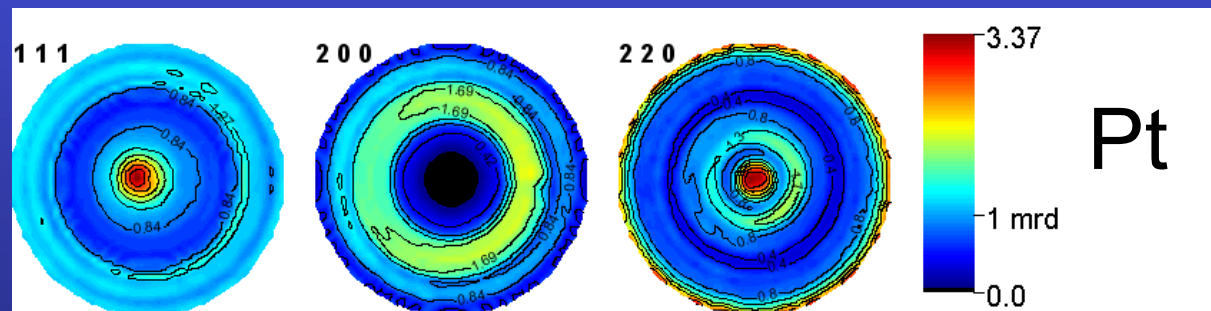
$T = 14270(3) \text{ nm}$

$\langle t \rangle = 2404(8) \text{ \AA}$

$\langle \varepsilon \rangle = 0.001853(2)$

$\sigma_{11} = -1019(2) \text{ MPa}$

$\sigma_{22} = -845(2) \text{ MPa}$



Rw (%) = 33.3

$a = 3.91198(1) \text{ \AA}$

$T = 1204(3) \text{ nm}$

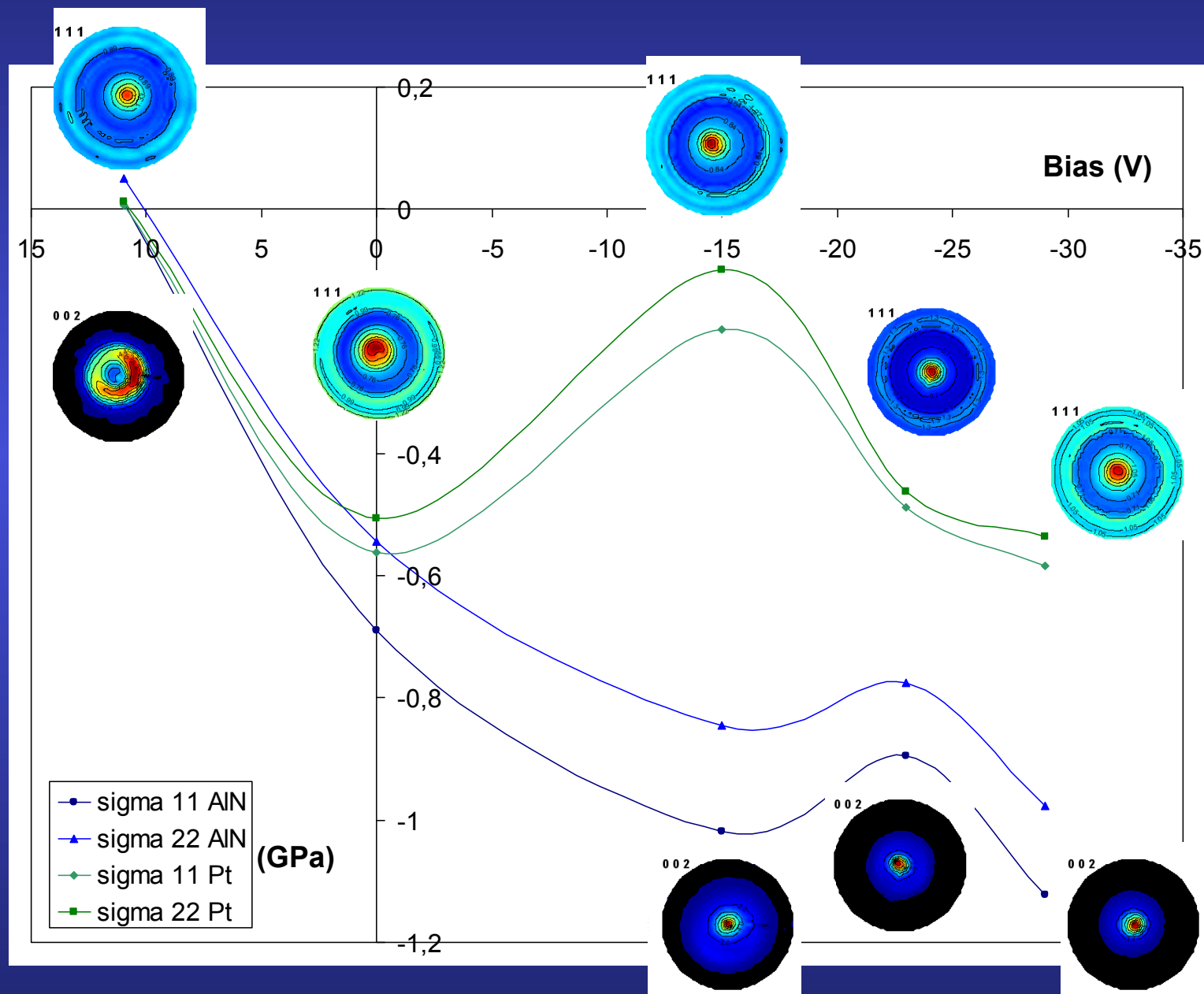
$\langle t \rangle = 2173(10) \text{ \AA}$

$\langle \varepsilon \rangle = 0.002410(3)$

$\sigma_{11} = -196.5(8)$

$\sigma_{22} = -99.6(6)$

Substrate bias vs stress-texture evolution



Si nanocrystalline thin films

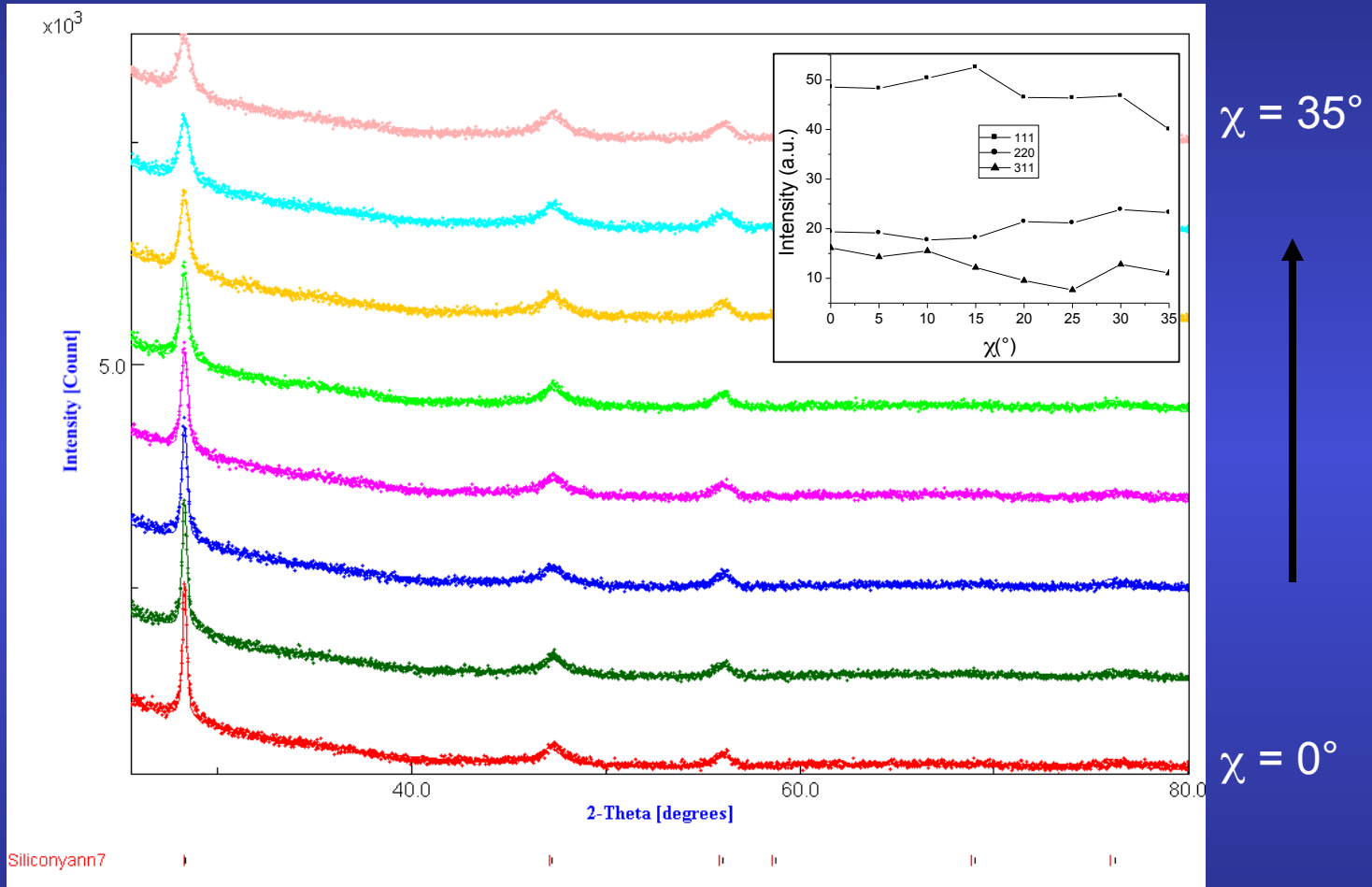
M. Morales, Caen

Silicon thin films deposition by reactive magnetron sputtering:

- ⇒ power density $2\text{W}/\text{cm}^2$
- ⇒ total pressure: $p_{\text{total}} = 10^{-1}$ Torr
- ⇒ plasma mixture: H_2 / Ar , $p_{\text{H}_2} / p_{\text{total}} = 80\%$
- ⇒ temperature: 200°C
- ⇒ substrates: amorphous SiO_2 (a- SiO_2)
(100)-Si single-crystals
- ⇒ target-substrate distance (d)
 - a- SiO_2 substrates: $d = 4, 6, 7, 8, 10, 12$ cm
films A, B, C, D, E, F
 - (100)-Si: $d = 6, 12$ cm
films G, H

Aim: quantum confinement, photoluminescence properties

Typical refinement

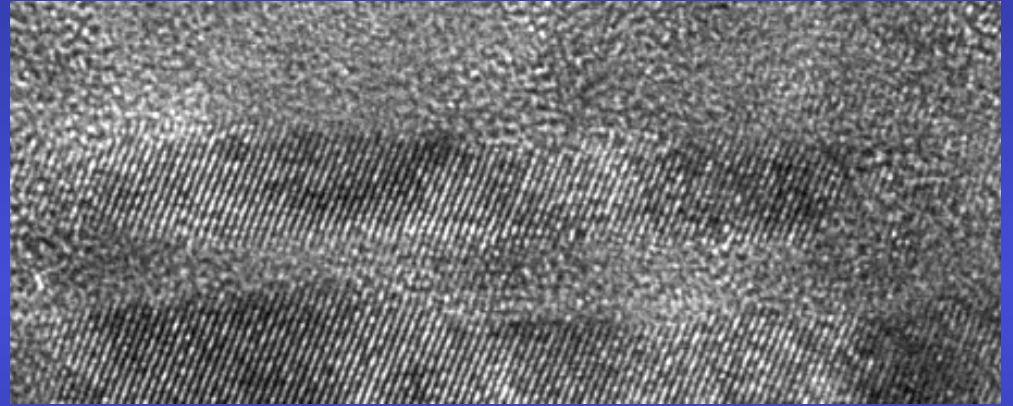
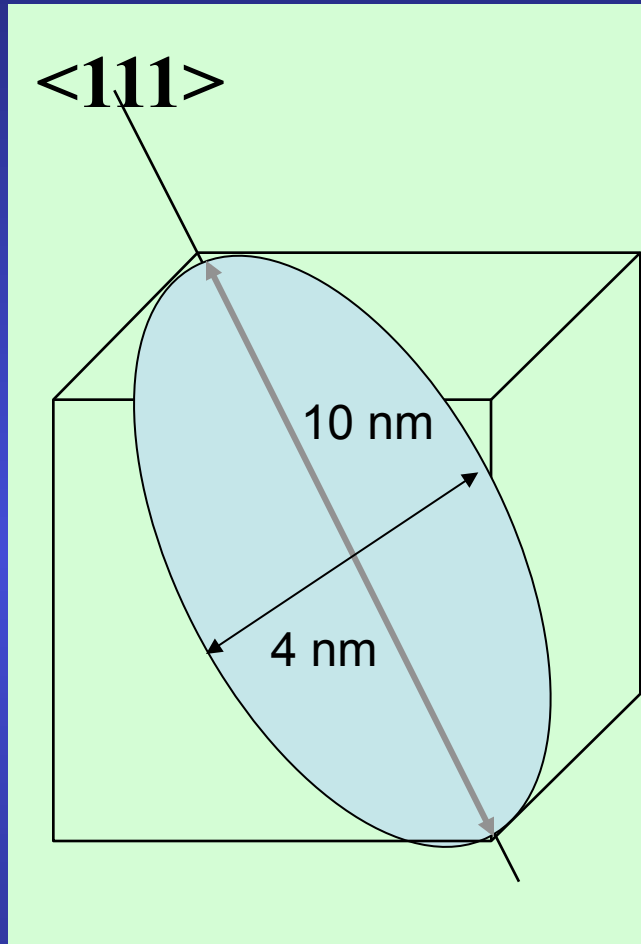


broad, anisotropic diffracted lines, textured samples

Refinement Results

Sample	d (cm)	a (Å)	RX thickness (nm)	Anisotropic sizes (Å)			Texture parameters			Reliability factors (%)			
				<111>	<220>	<311>	Maximum (m.r.d.)	minimum (m.r.d.)	Texture index F ² (m.r.d ²)	RP ₀	R _w	R _B	R _{exp}
A	4	5.4466 (3)	—	94	20	27	1.95	0.4	1.12	1.72	4.0	3.7	3.5
B	6	5.4439 (2)	711 (50)	101	20	22	1.39	0.79	1.01	0.71	4.9	4.3	4.2
C	7	5.4346 (4)	519 (60)	99	40	52	1.72	0.66	1.05	0.78	4.3	4.0	3.9
D	8	5.4461 (2)	1447 (66)	100	22	33	1.57	0.63	1.04	0.90	5.5	4.6	4.5
E	10	5.4462 (2)	1360 (80)	98	20	25	1.22	0.82	1.01	0.56	5.0	3.9	4.0
F	12	5.4452 (3)	1110 (57)	85	22	26	1.59	0.45	1.05	1.08	4.2	3.5	3.7
G	6	5.4387 (3)	1307 (50)	89	22	28	1.84	0.71	1.01	1.57	5.2	4.7	4.2
H	12	5.4434 (2)	1214 (18)	88	22	24	2.77	0.50	1.12	2.97	5.0	4.5	4.3

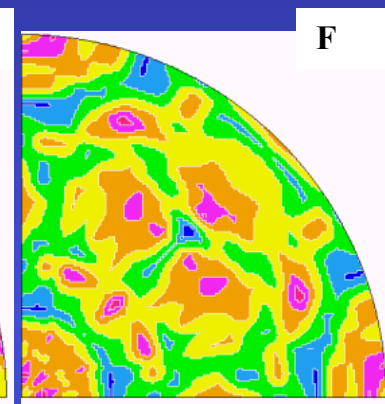
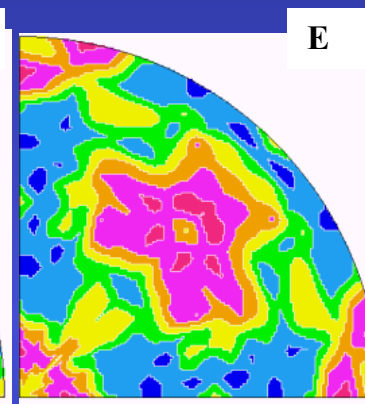
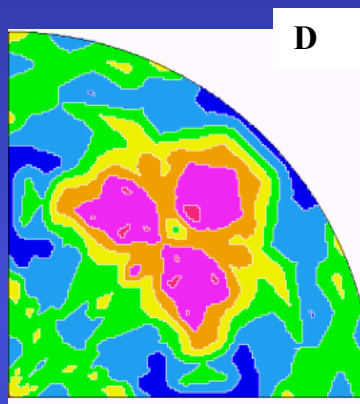
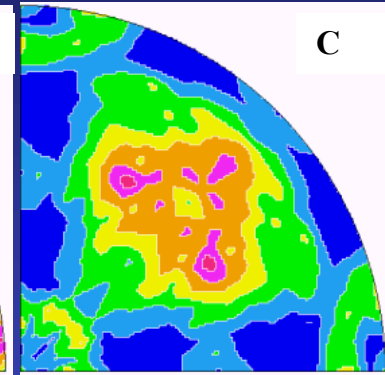
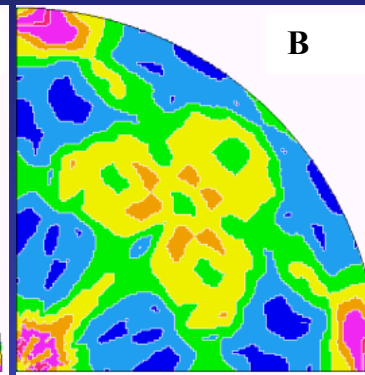
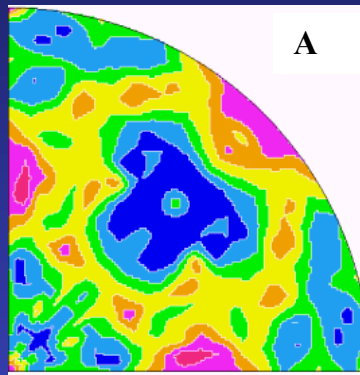
Mean anisotropic shape



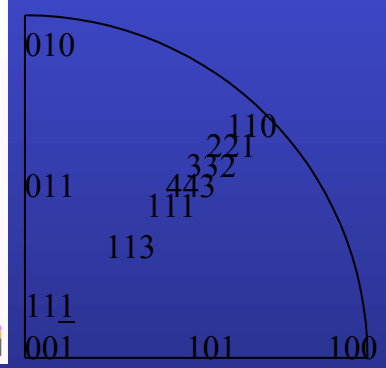
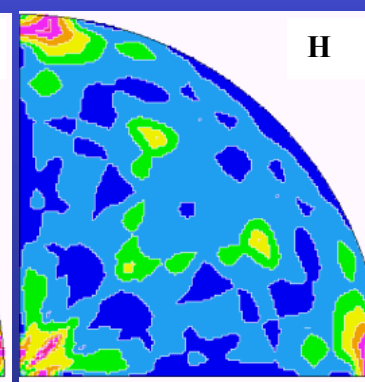
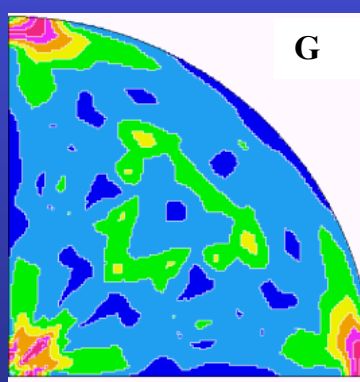
Schematic of the mean crystallite shape for Sample D represented in a cubic cell, as refined using the Popa approach and exhibiting a strong elongation along $\langle 111 \rangle$, and TEM image

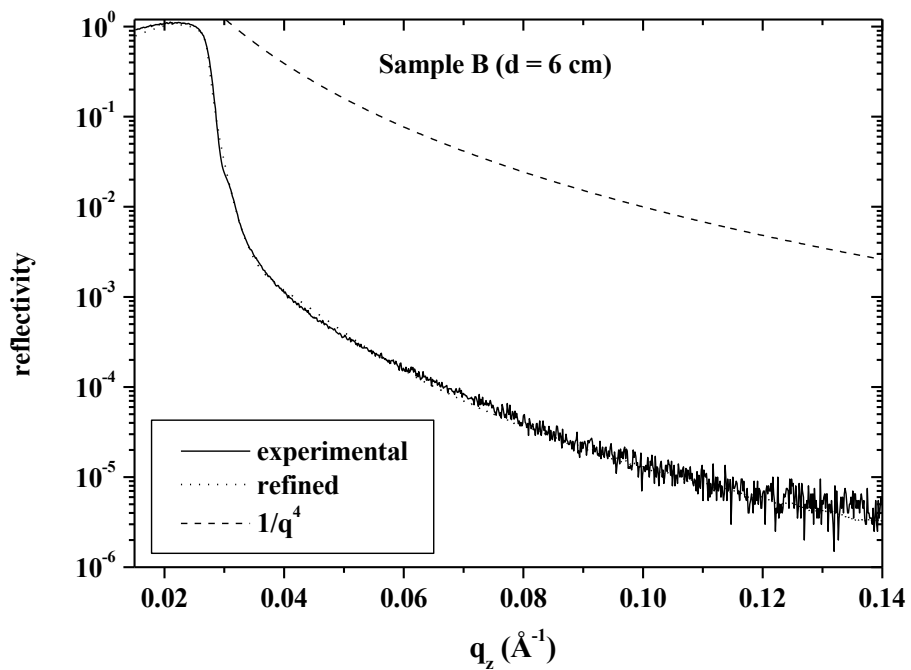
001 Inverse Pole Figures

a-SiO₂



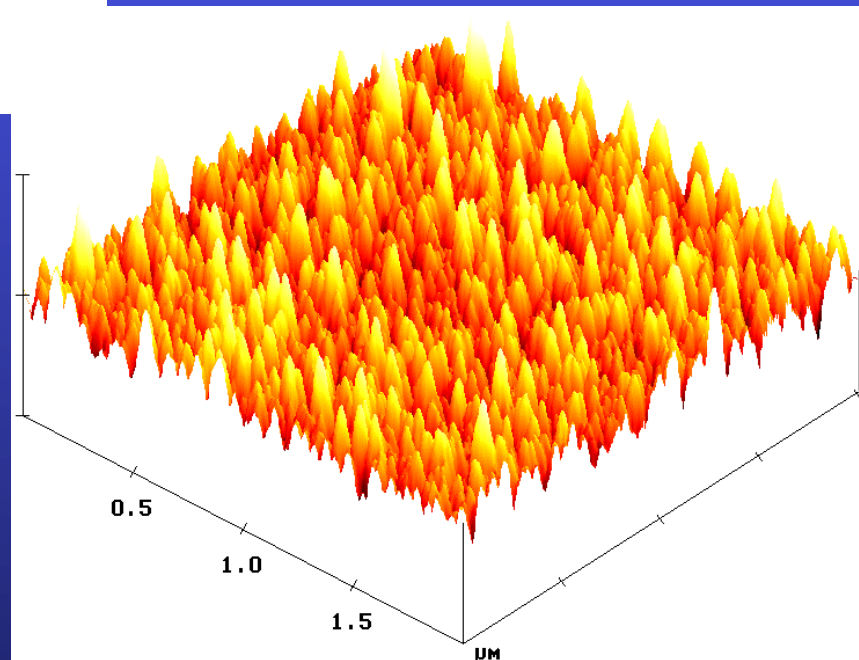
(100)-Si

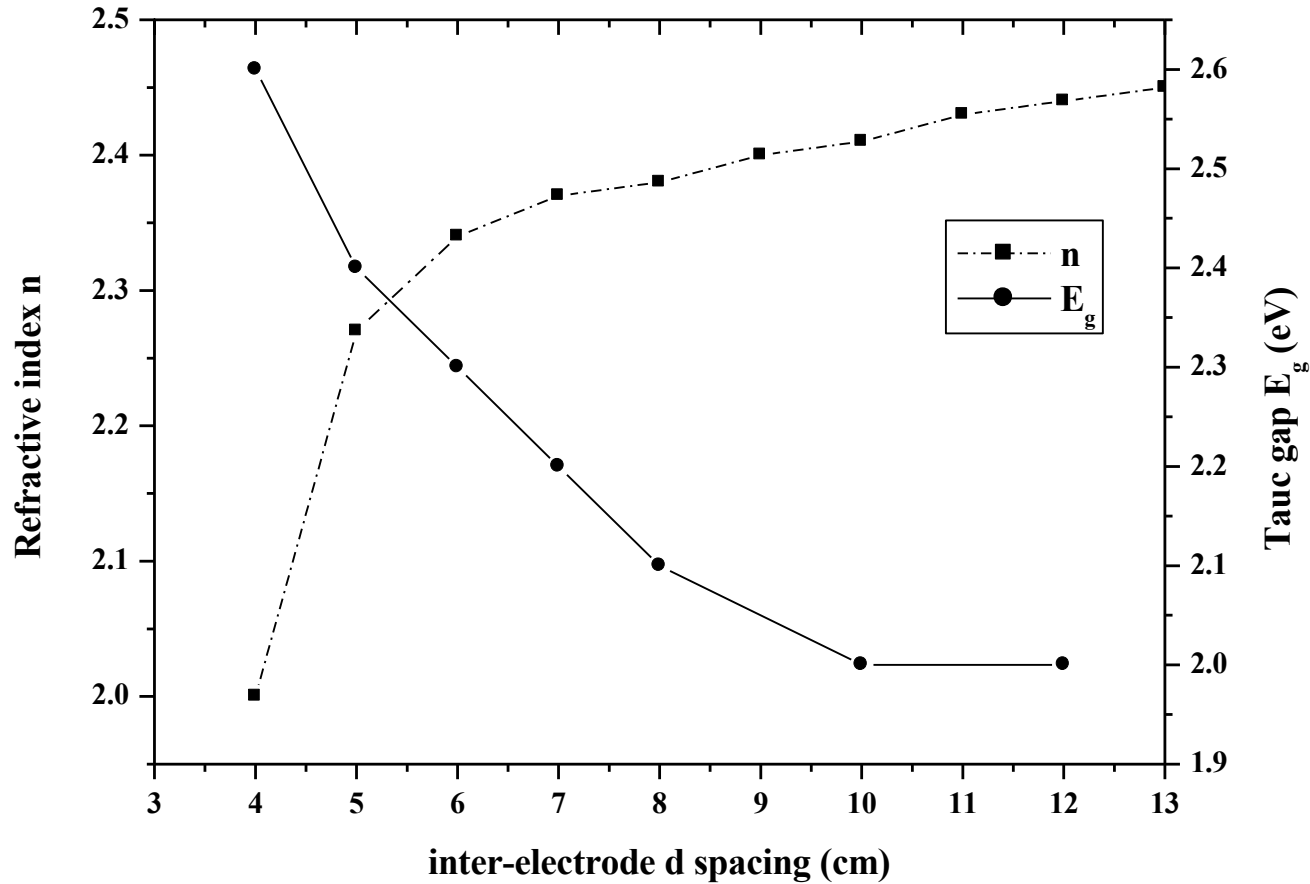




XRR:
Roughness
governed

AFM:
homogeneous
roughness

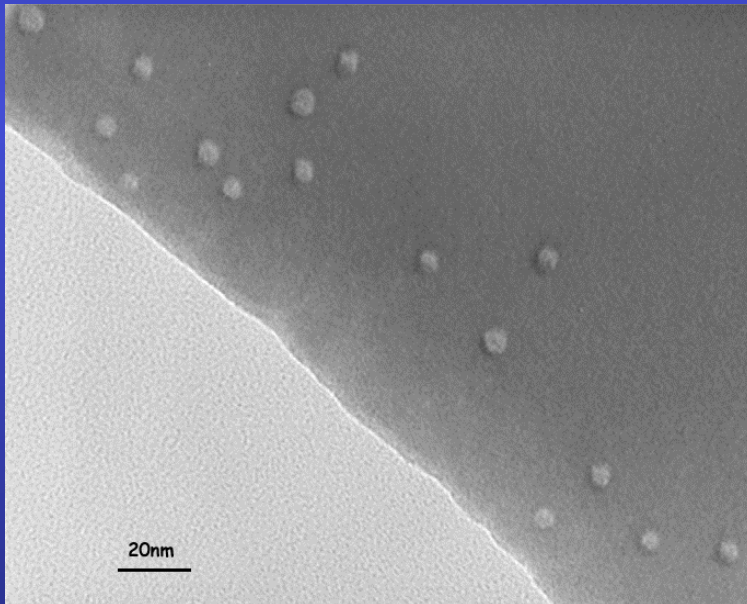




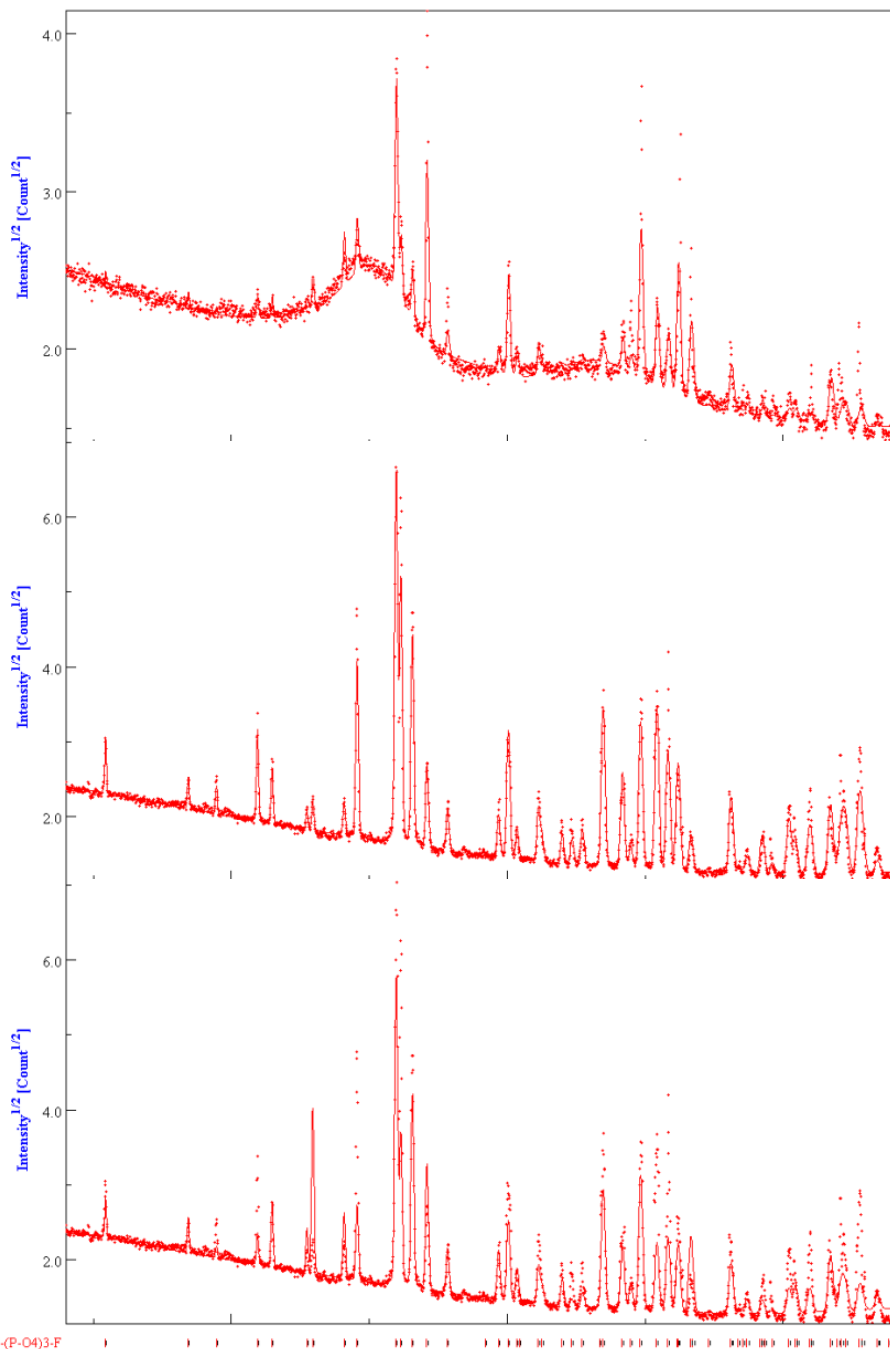
↪ Refractive index linked to film porosities:
 Larger target-sample distances: increased compacity due to lower
 nanopowder filling

Irradiated FluorApatite (FAp) ceramics

Self-recrystallisation under irradiation, depending on $\text{SiO}_4 / \text{PO}_4$ ratio (FAp / Nd-Britholite) and on irradiating species



TEM of FAp
irradiated with 70
MeV, 10^{12} Kr cm^{-2}
ions



texture corrected,
 10^{13} Kr cm⁻²

Virgin, with texture
correction

Virgin, no texture
correction

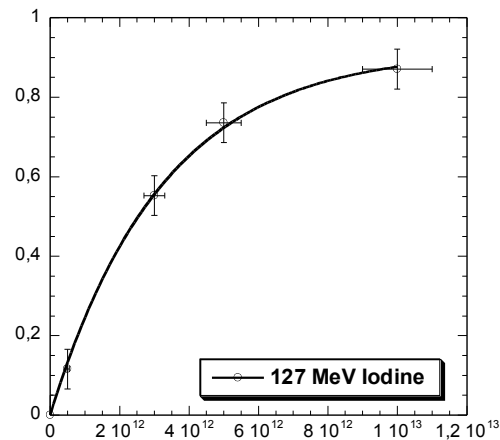
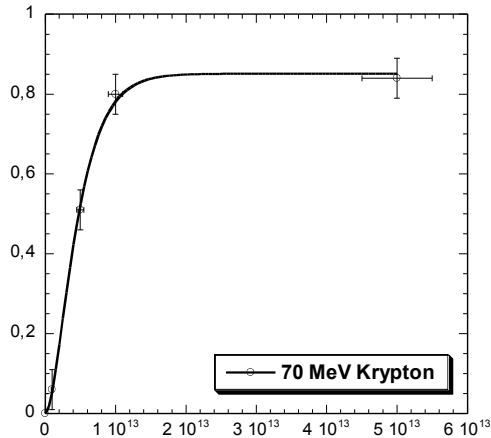
Fluence (ions.cm ⁻²)	Vc/V (%)	A (Å)	c (Å)	<t> (nm)	Δ _a /a ₀ (%)	Δ _c /c ₀ (%)	R _w (%)	R _B (%)
0	100	9.3365(3)	6,8560(5)	294(22)	-	-	14.6	9.1
Kr								
10 ¹¹	100	-	-	-	-	-		
10 ¹²	100	-	-	-	-	-		
5.10 ¹²	49(1)	9.3775(9)	6.8912(8)	294(20)	0.44	0.53	24	15
10 ¹³	20(1)	9.4236(5)	6.9105(5)	291(20)	0.94	0.82	9.9	6
5.10 ¹³	14(1)	9.3160(4)	6.8402(5)	294(22)	-0.21	-0.22	10.5	5.9
I								
10 ¹¹	-	-	-	-	-	-		
5.10 ¹¹	86(2)	9.3603(3)	6.8790(5)	90(10)	0.26	0.35	23.9	15.1
10 ¹²	-	-	-	-	-	-		
3.10 ¹²	47(2)	9.3645(3)	6.8840(5)	91(6)	0.30	0.42	13.3	9
5.10 ¹²	29.2(5)	9.3765(5)	6.8881(6)	77(11)	0.44	0.48	10.4	7.3
10 ¹³	13.2(2)	9.3719(4)	6.8857(6)	82(9)	0.38	0.45	6.7	4.9

Single impact model associated to crystal size reduction

Cell parameters and volume increase, then relax

Amorphisation / recrystallisation competition: single or double impact

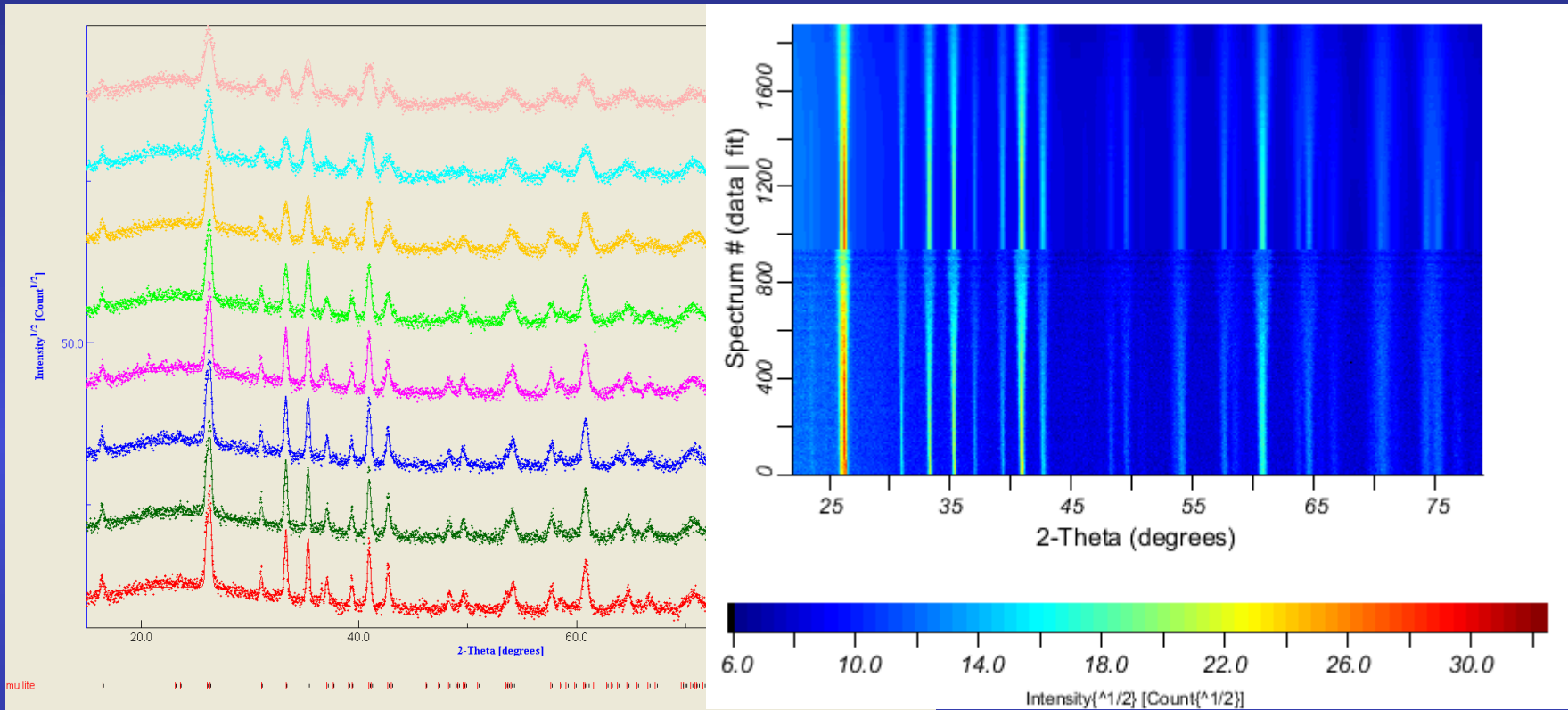
Amorphous/crystalline volume fraction (damaged fraction $F_d = V_a / V$) as determined by x-ray diffraction



B

Fitting parameters	Krypton		Iodine
	Single impact $F_d = B(1 - \exp(-A\phi t))$	Double impact $F_d = B(1 - (1 + A\phi t) \exp(-A\phi t))$	Single impact $F_d = B(1 - \exp(-A\phi t))$
$A = \pi R^2$ (cm ²)	$1.85 \pm 0.15 \cdot 10^{-13}$	$4.1 \pm 0.15 \cdot 10^{-13}$	$3.3 \pm 0.15 \cdot 10^{-13}$
Radius R (nm)	2.4 ± 0.2	3.6	3.2
B (Max.damage rate)	0.87	0.85 ± 0.2	0.92 ± 0.2
χ^2	0.013	0.0006	0.0004

Mullite-silica composites

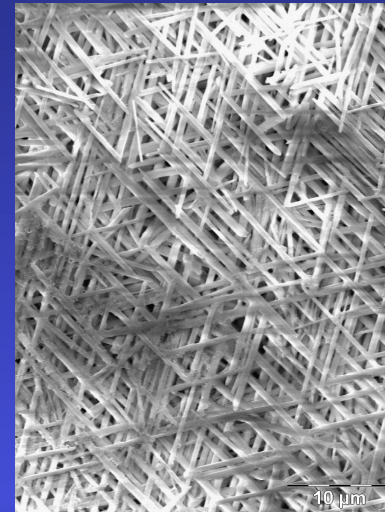
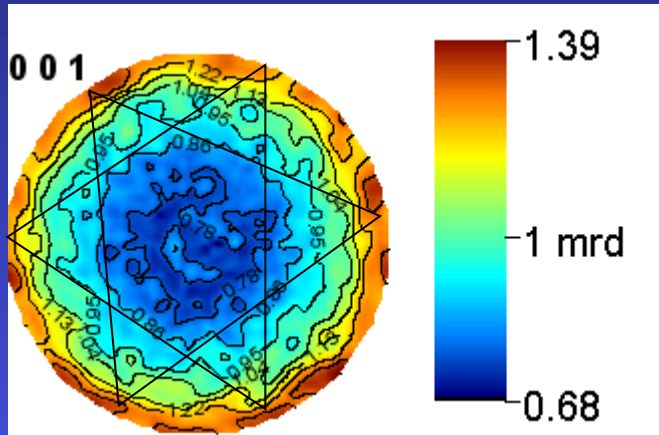


ODF: $R_w = 4.87 \%$, $R_B = 4.01 \%$

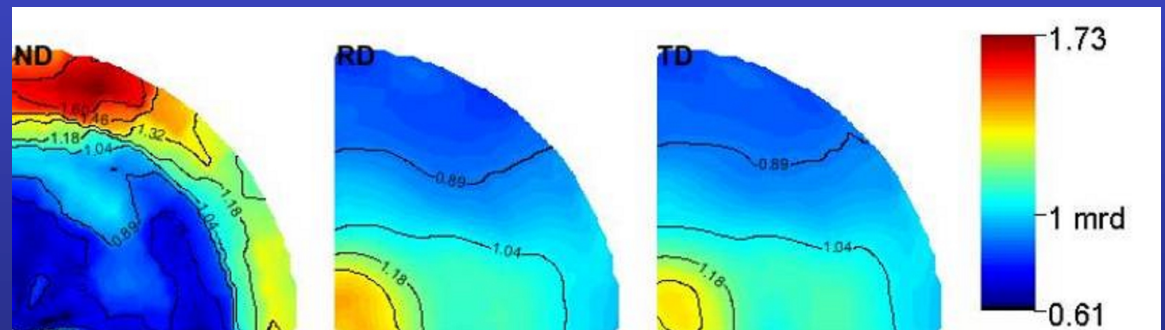
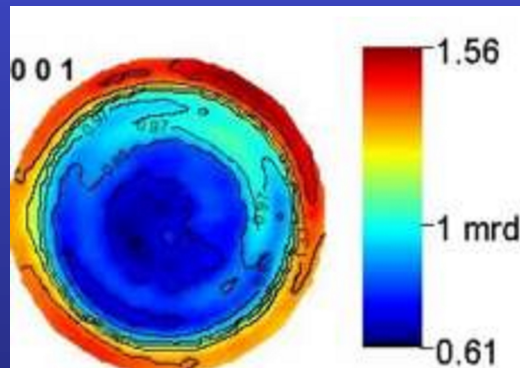
Rietveld: $R_w = 12.90 \%$, GoF = 1.77

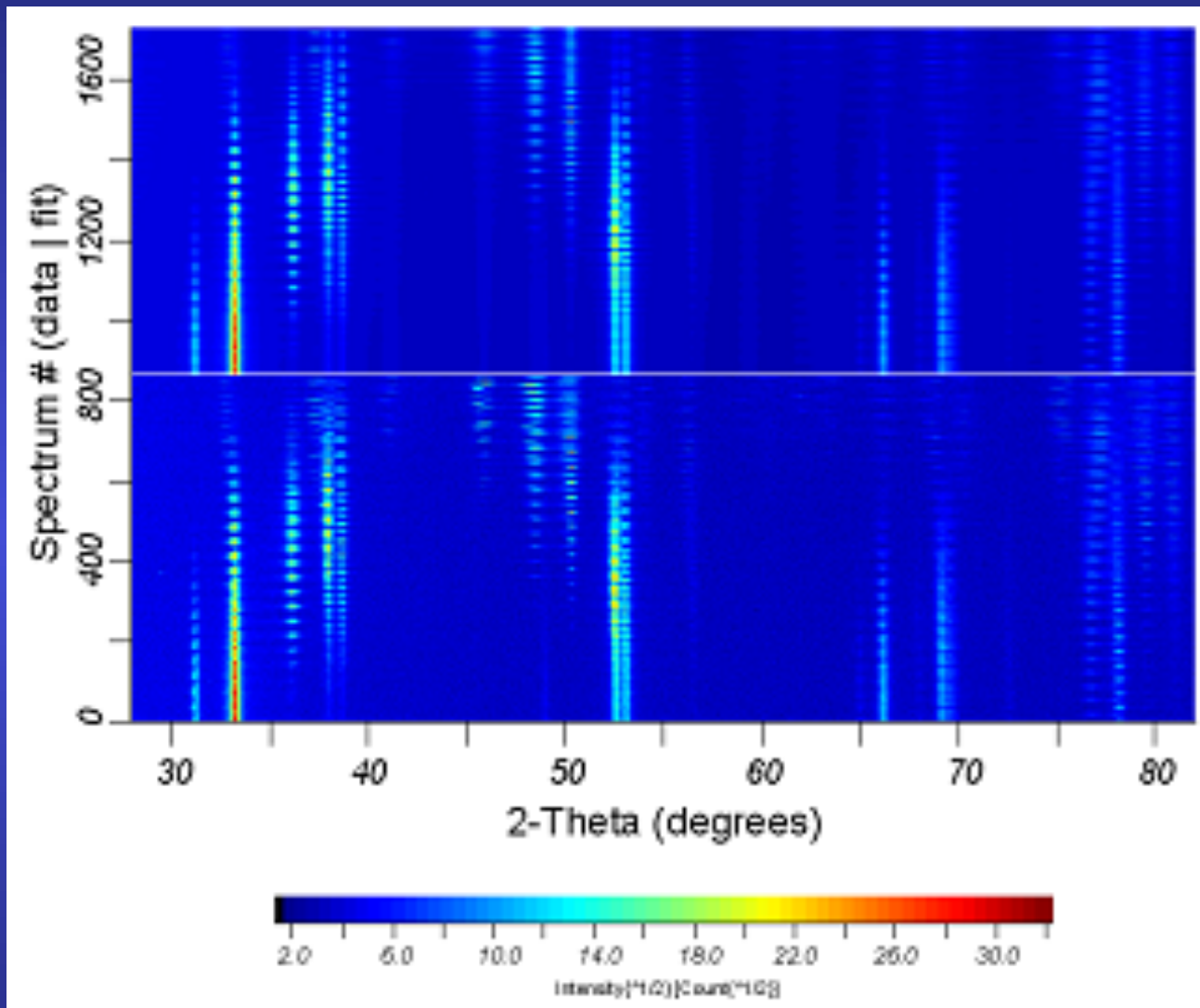
Mullite: $a = 7.56486(5) \text{ \AA}$; $b = 7.71048(5) \text{ \AA}$; $c = 2.89059(1) \text{ \AA}$

Uniaxially pressed



Centrifugated





refined

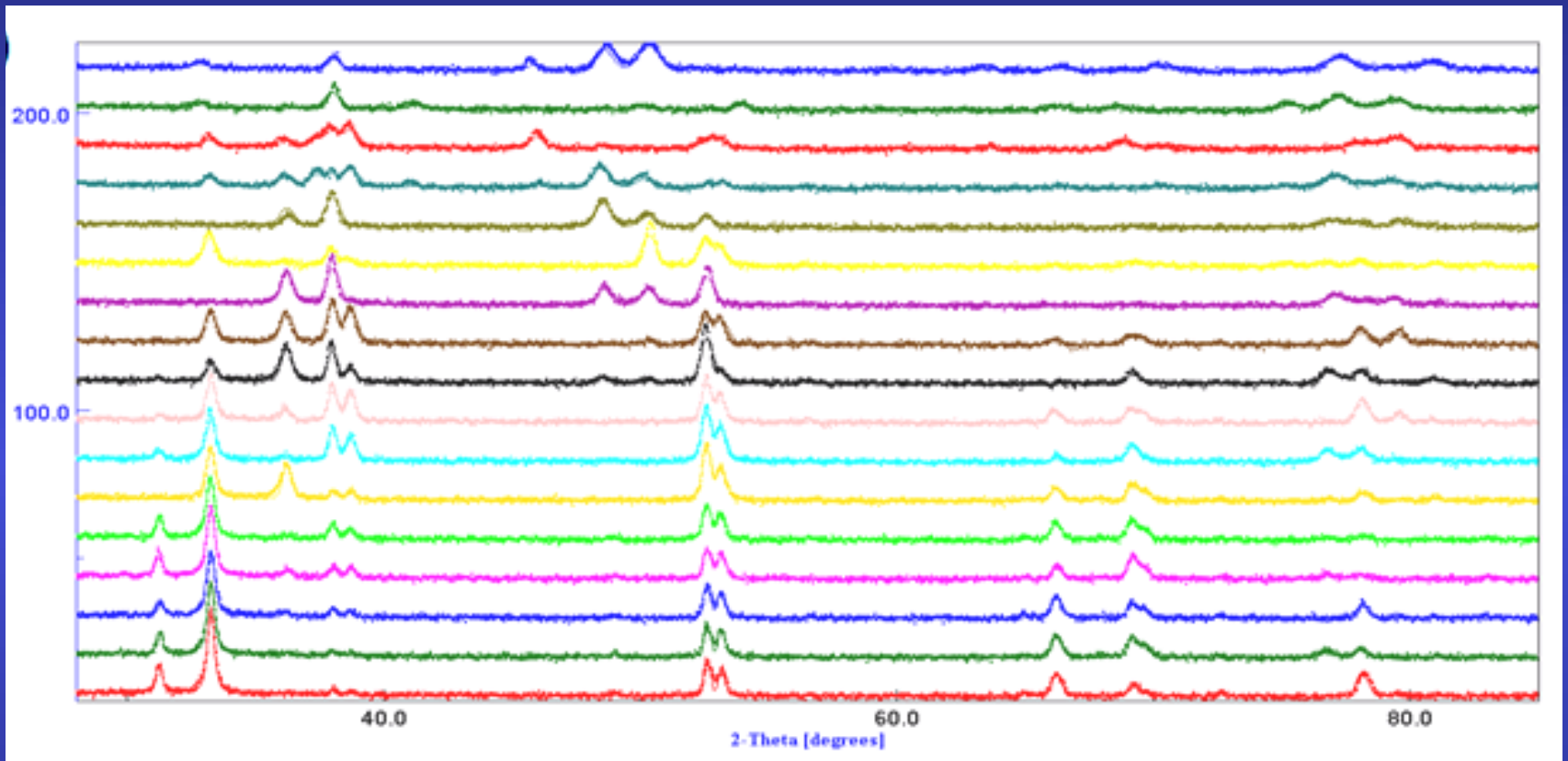
experiments

GoF:1,72

R_w: 28,0%

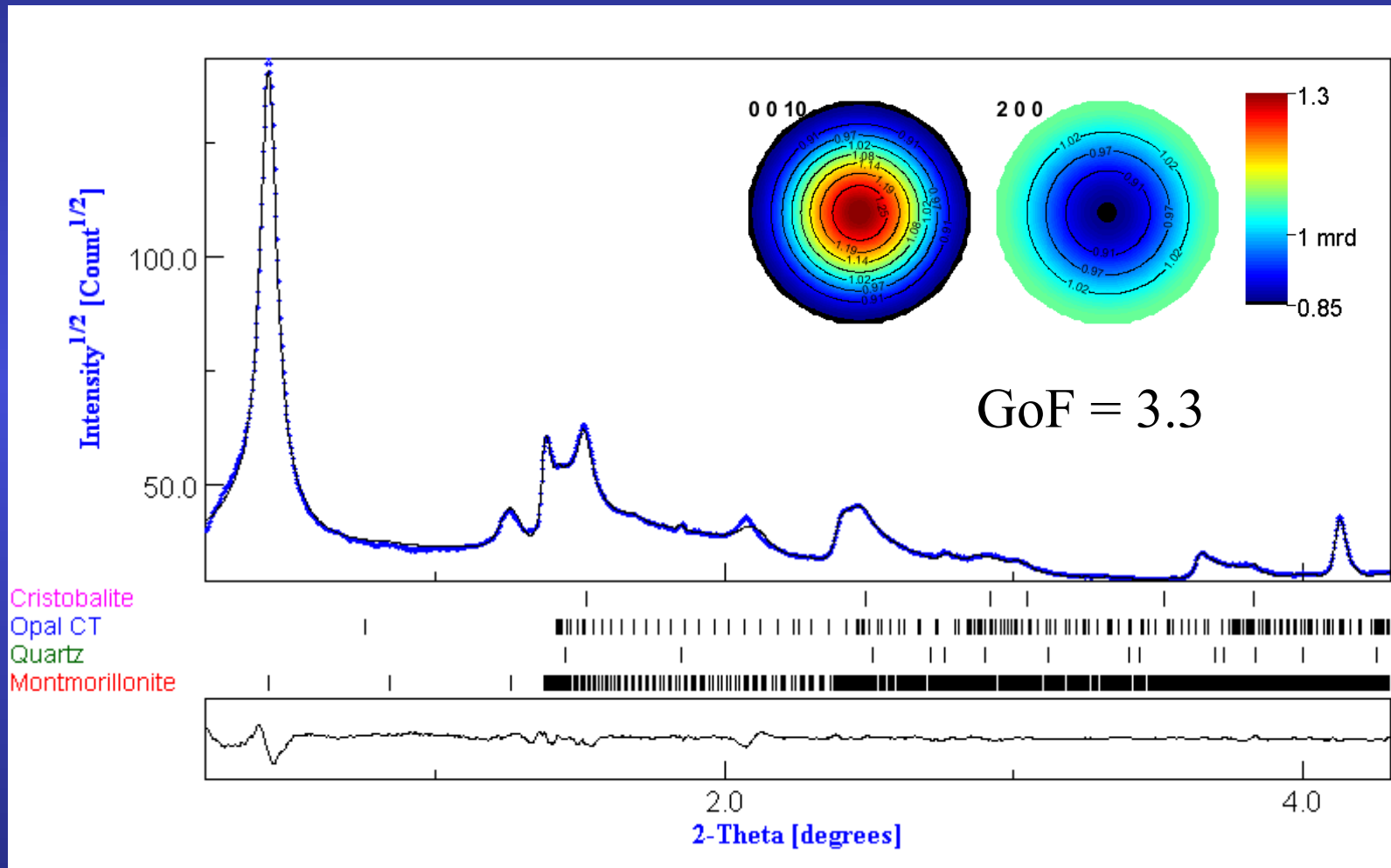
R_{exp}:21,3%

for all (χ, φ) sample orientations



IRC layer of *Charonia lampas lampas* for selected (χ, φ) sample orientations

Turbostratic phyllosilicate aggregates



Specular reflectivity: $\mathbf{q}=(0,0,z)$

- Fresnel:

$$R(\mathbf{q}) = \left| \frac{q_z - \sqrt{q_z^2 - q_c^2 + \frac{32i\pi^2\beta}{\lambda^2}}}{q_z + \sqrt{q_z^2 - q_c^2 + \frac{32i\pi^2\beta}{\lambda^2}}} \right|^2 \delta q_x \delta q_y$$

- matrix:

$$R^{flat} = \frac{r_{0,1}^2 + r_{1,2}^2 + 2r_{0,1}r_{1,2} \cos 2k_{z,1}h}{1 + r_{0,1}^2 r_{1,2}^2 + 2r_{0,1}r_{1,2} \cos 2k_{z,1}h}$$

- Born approximation:
Electron Density Profile

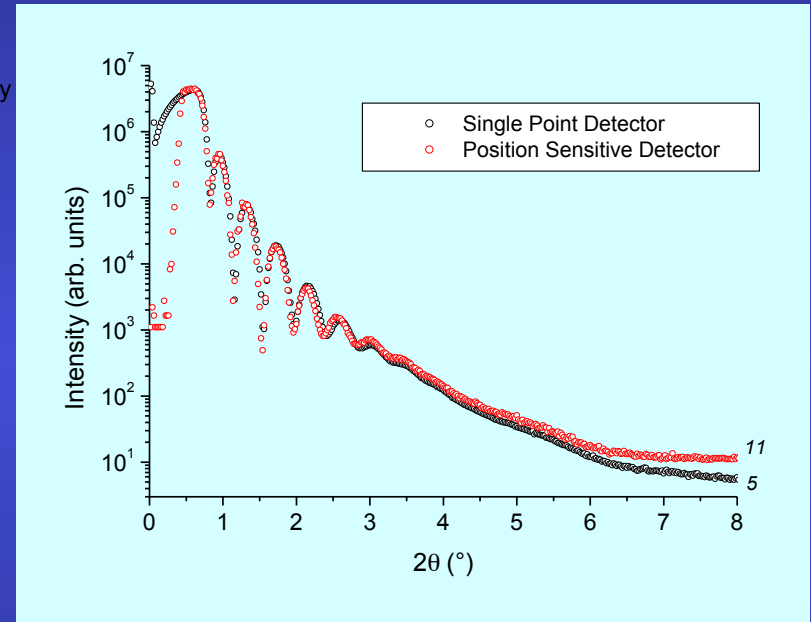
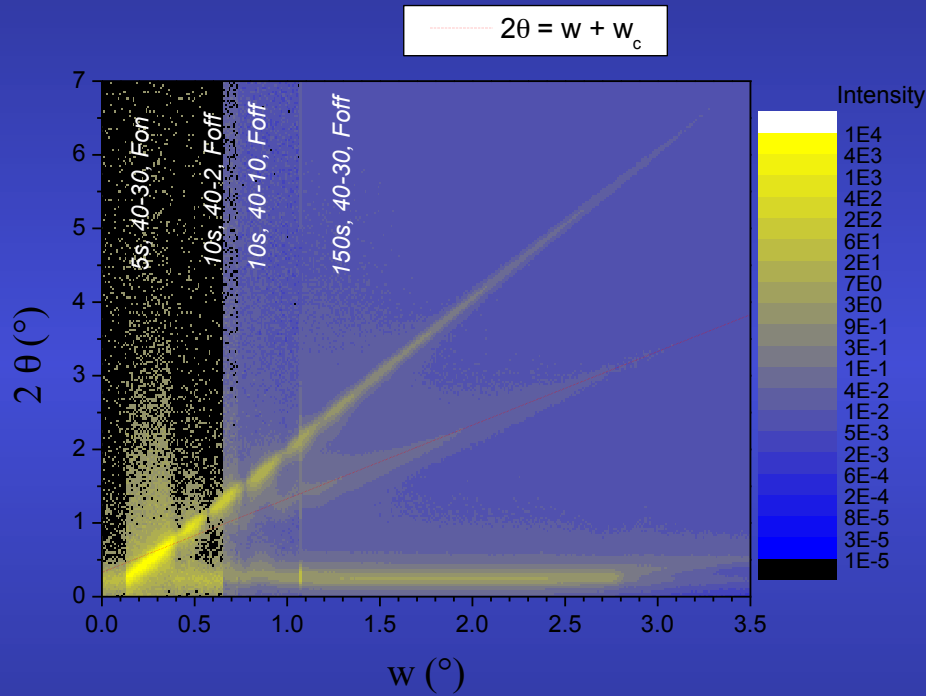
$$R(q_z) = r \cdot r^* = R_F(q_z) \left| \frac{1}{\rho_s} \int_{-\infty}^{+\infty} \frac{d\rho(z)}{dz} e^{iq_z z} dz \right|^2$$

- Roughness:

$$R^{rough}(q_z) = R(q_z) \exp(-q_{z,0} q_{z,1} \sigma^2) \quad \text{Low-angles (reflectivity)}$$

$$S_R = 1 - p \exp(-q) + p \exp\left(\frac{-q}{\sin \theta}\right) \quad \text{high-angle (Suortti)}$$

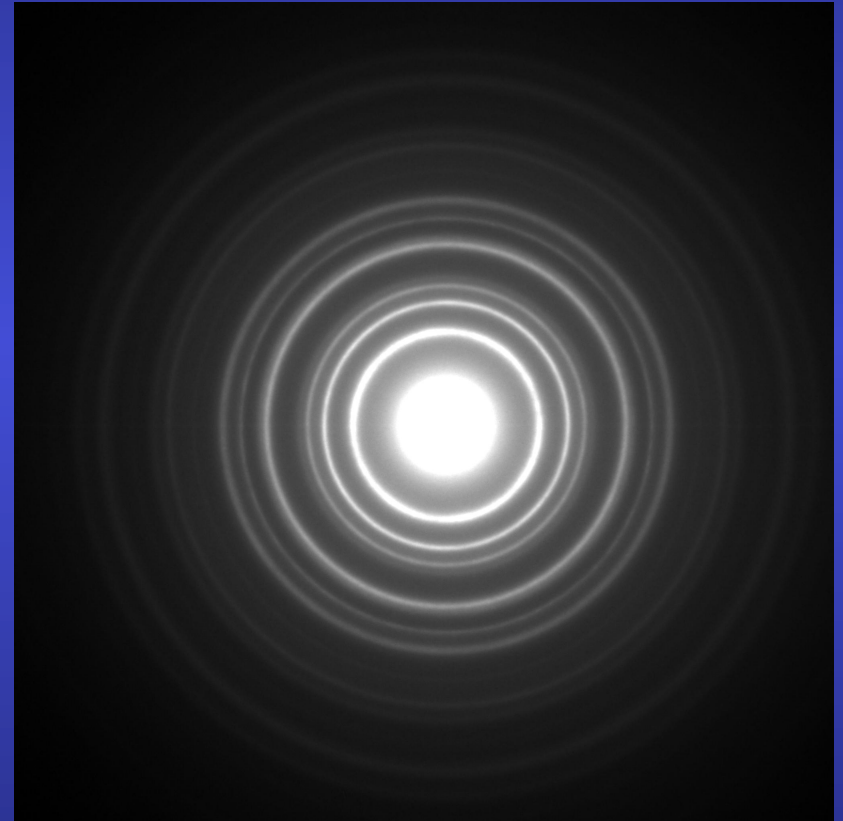
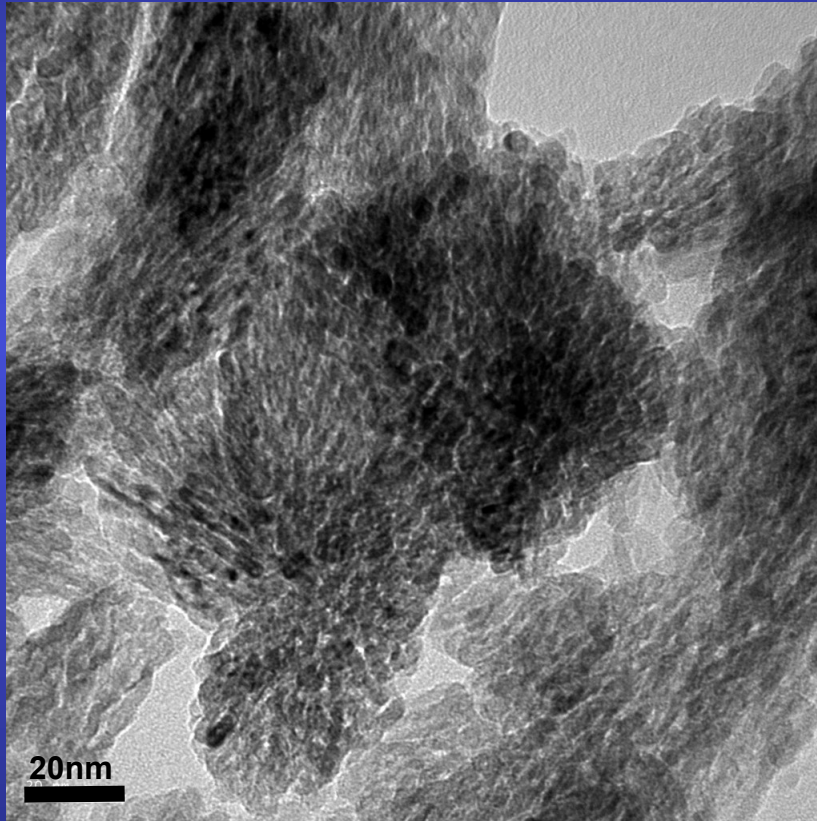
CPS scans

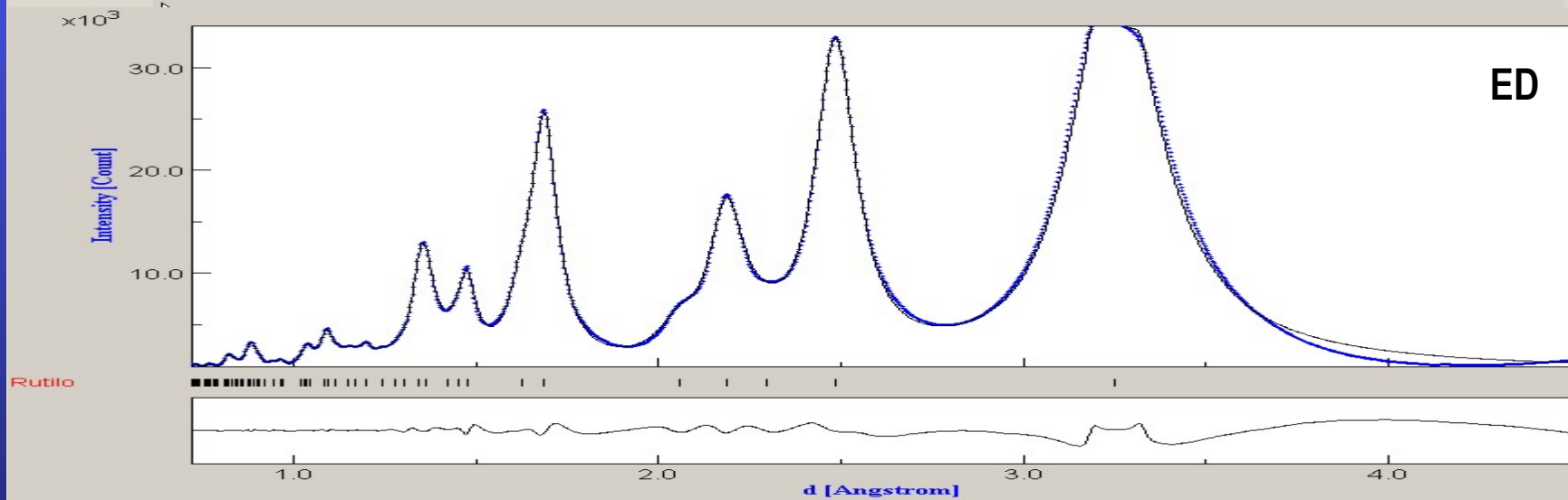
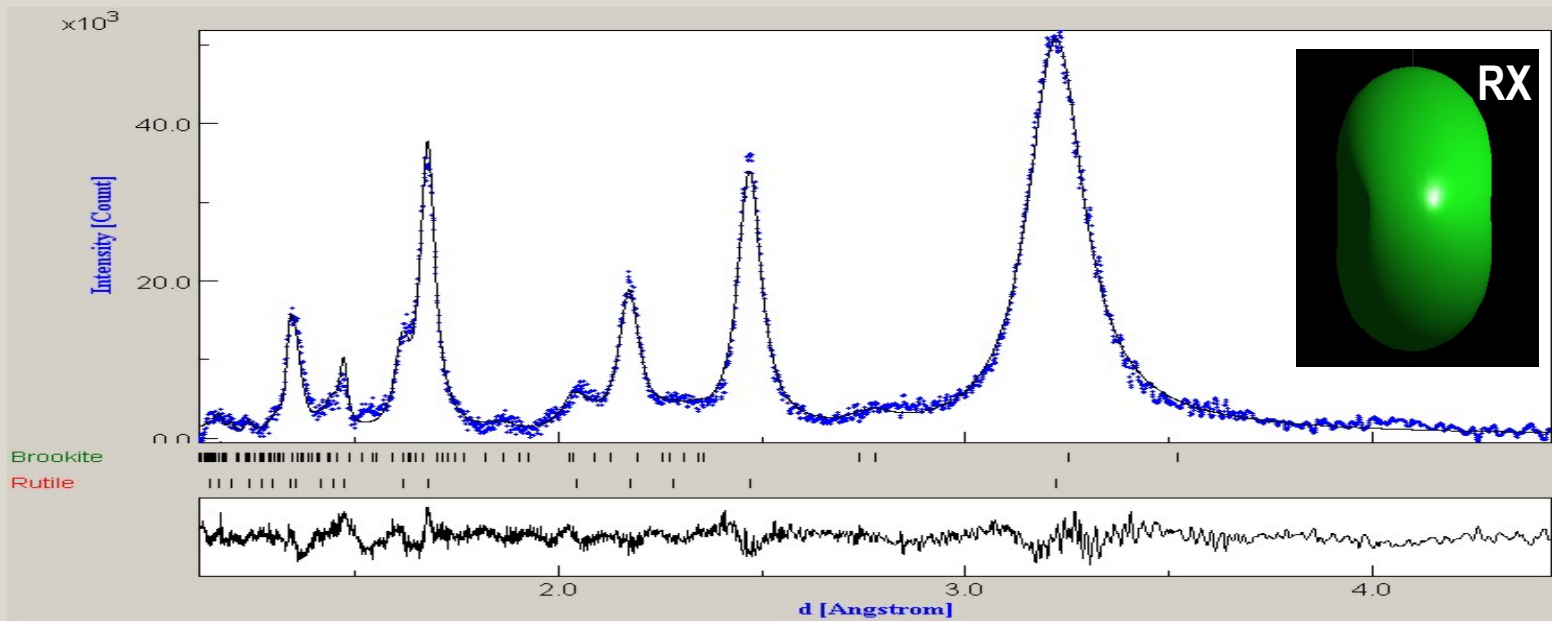


Useful for having bot specular and off-specular signals in one scan

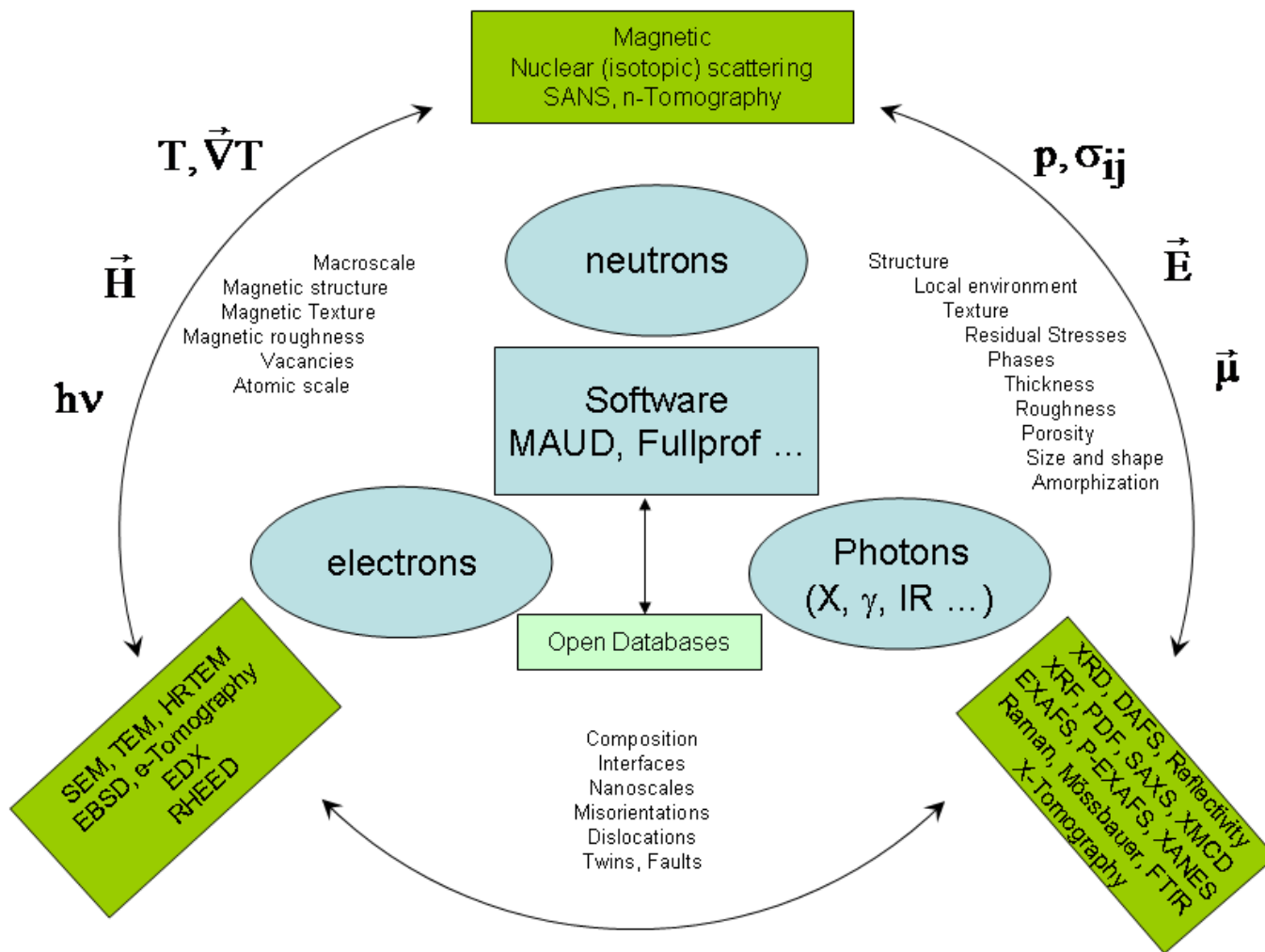
Microstructure of nanocrystalline materials: TiO_2 rutile ⁽¹⁾

- ▶ *quantitative analysis of electron diffraction ring pattern ?*





Why not more ?



Conclusions

- a) A lot of dilemma are only apparent
- b) Texture helps to resolve them: good for real samples
- c) Anisotropy favours higher resolutions
- d) Combined analysis may be a solution, unless you can destroy your sample or are not interested in macroscopic anisotropy ...
- e) If you think you can destroy it, perhaps think twice
- f) more information is always needed: why not more?
- g) Combined Analysis (D. Chateigner Ed), Wiley-ISTE 2010